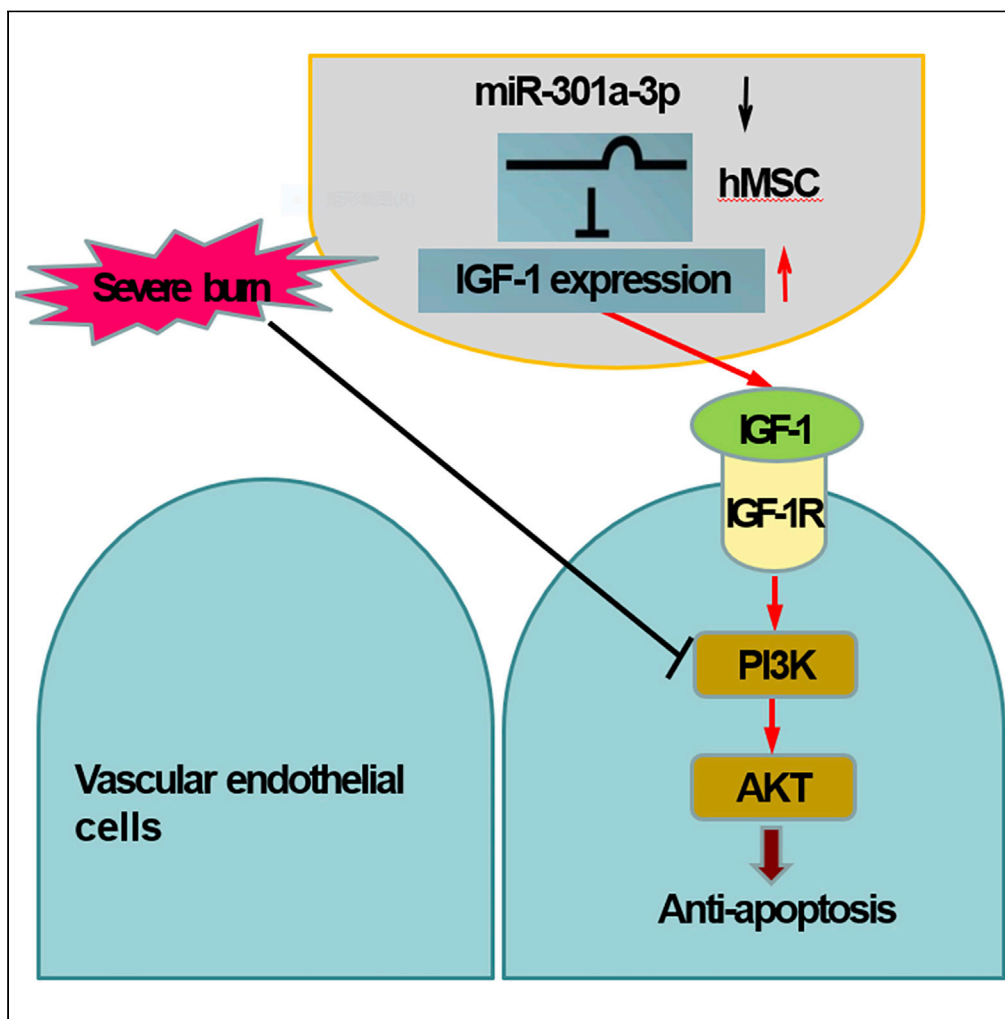


Article

Down-Regulation of miR-301a-3p Reduces Burn-Induced Vascular Endothelial Apoptosis by potentiating hMSC-Secreted IGF-1 and PI3K/Akt/FOXO3a Pathway



Lingying Liu,
Huinan Yin,
Xingxia Hao, ...,
Hailiang Bai,
Xiuxiu Shi,
Shaозeng Li

cyj304@126.com

HIGHLIGHTS

IGF-1 secreted by hMSC suppressed severe burn-induced apoptosis of HUVECs

miR-301a-3p directly regulated IGF-1 synthesis and secretion in hMSC

Downregulation of miR-301a-3p protected against multiple organ dysfunction

miR-301a-3p regulated PI3K/Akt/FOXO3 signaling through hMSC-secreted IGF-1

Liu et al., iScience 23, 101383
August 21, 2020 © 2020
<https://doi.org/10.1016/j.isci.2020.101383>



Article

Down-Regulation of miR-301a-3p Reduces Burn-Induced Vascular Endothelial Apoptosis by potentiating hMSC-Secreted IGF-1 and PI3K/Akt/FOXO3a Pathway

Lingying Liu,^{1,2,3,9} Huinan Yin,^{2,9} Xingxia Hao,^{3,9} Huifeng Song,^{2,9} Jiake Chai,^{2,8,10,*} Hongjie Duan,² Yang Chang,² Longlong Yang,² Yushou Wu,² Shaofang Han,² Xiaoteng Wang,² Xiaotong Yue,² Yunfei Chi,² Wei Liu,² Qiong Wang,⁴ Hongyu Wang,⁴ Hailiang Bai,⁵ Xiuxiu Shi,⁶ and Shaozeng Li⁷

SUMMARY

Vascular endothelium dysfunction plays a pivotal role in the initiation and progression of multiple organ dysfunction. The mesenchymal stem cell (MSC) maintains vascular endothelial barrier survival via secreting bioactive factors. However, the mechanism of human umbilical cord MSC (hMSC) in protecting endothelial survival remains unclear. Here, we found IGF-1 secreted by hMSC suppressed severe burn-induced apoptosis of human umbilical vein endothelial cells (HUVECs) and alleviated the dysfunction of vascular endothelial barrier and multiple organs in severely burned rats. Severe burn repressed miR-301a-3p expression, which directly regulated IGF-1 synthesis and secretion in hMSC. Down-regulation of miR-301a-3p decreased HUVECs apoptosis, stabilized endothelial barrier permeability, and subsequently protected against multiple organ dysfunction *in vivo*. Additionally, miR-301a-3p negatively regulated PI3K/Akt/FOXO3 signaling through IGF-1. Taken together, our study highlights the protective function of IGF-1 against the dysfunction of multiple organs negatively regulated by miR-301a-3p, which may provide the theoretical foundation for further clinical application of hMSC.

INTRODUCTION

Severe burn is a complex and severe traumatic injury with high mortality in the acute phase (Auger et al., 2017; Liu et al., 2016). Vascular endothelial barrier dysfunction induced by severe burn, synergism of excessive inflammation, and serious metabolic disturbance are important contributors for the development of multiple organ dysfunction, such as acute kidney injury (AKI), cardiac dysfunction, and multiple organ failure (MOF) (Lam et al., 2018; Haines et al., 2017). It has been demonstrated that apoptosis of vascular endothelial cells induced by severe burn is one of the main concerns responsible for vascular endothelial barrier dysfunction at the early stage (Tian et al., 2015). Therefore, reducing vascular endothelial cells apoptosis may benefit patients with endothelial barrier disorder and multiple organ dysfunction post severe burn.

Because of its lower immunogenicity and higher proliferation rate, human umbilical cord mesenchymal stem cell (hMSC) is considered as a perfect candidate for stem cell-based therapy and regenerative medicine (Matthay et al., 2017; Lee and Wang, 2017; Laroye et al., 2017). Increasing evidence has shown that hMSC can protect the endothelial barrier function and effectively treat ill surgical patients who develop multiple organ dysfunction post severe burn and traumatic brain injury (TBI) (Dorransoro and Robbins, 2013; Pati et al., 2015; Menger et al., 2012). The beneficial effects of hMSC are partially explained by secretion of bioactive factors, such as anti-apoptotic factors, immunomodulation factors, antioxidant factors, and exosomes (Yin et al., 2019; Temnov et al., 2018; Beltran et al., 2015). Among these bioactive factors, insulin-like growth factor (IGF-1) is an important anti-apoptotic factor that regulates cell survival (Li et al., 2017; Song et al., 2016). Bake et al. showed that IGF-1 could be beneficial to the endothelial barrier function at the earliest phase of ischemia (Bake et al., 2019). Pati et al. suggested that bone marrow MSC preserved vascular endothelial integrity in the lungs after hemorrhagic shock (Pati et al., 2011). Our previous study also showed that IGF-1 was one of the most important factors secreted by hMSC in eliminating apoptosis in

¹Nutrition Department, the Fourth Medical Center Affiliated to PLA General Hospital, Beijing 100037, China

²Burns Institute of PLA, Department of Burn & Plastic Surgery, the Fourth Medical Center Affiliated to PLA General Hospital, Beijing 100037, China

³College of Basic Medicine, the Inner Mongolia Medical University, Hohhot, 010110, Inner Mongolia, China

⁴Department of Burn Surgery, the Third Affiliated Hospital of Inner Mongolia Medical University (Inner Mongolia BaoGang Hospital), Baotou 014010, Inner Mongolia, China

⁵Department of Plastic Surgery, The Second Hospital, Shanxi Medical University, Taiyuan 030001, Shanxi Province, China

⁶Department of Orthopedic Rehabilitation, the Fourth Medical Center Affiliated to PLA General Hospital, Beijing, 100037, China

⁷Department of Clinical Laboratory, the Fourth Medical Center Affiliated to PLA General Hospital, Beijing 100037, China

⁸Present address: Department of Burn & Plastic Surgery, the Fourth Medical Center Affiliated to PLA General Hospital, No.51 Fucheng Road, Haidian District Beijing 100048, China

⁹These authors contributed equally

¹⁰Lead Contact

*Correspondence: cjk304@126.com

<https://doi.org/10.1016/j.isci.2020.101383>



severely burned wound (Liu et al., 2014). However, the mechanism of IGF-1 secreted by hMSC on protecting endothelial survival and function remains unclear.

MicroRNAs (miRNAs) are 21–24 nucleotides noncoding RNAs that negatively regulate the expression of genes by binding to the 3' untranslated regions (3' UTRs) (Zhao and Srivastava, 2007; Kertesz et al., 2007; Wu and Belasco, 2008). MiRNAs participate in multiple cellular processes, including differentiation and organogenesis, as well as a broad array of repair and regeneration mechanisms of MSC (Huang et al., 2013; Lakshmiopathy and Hart, 2008; Wen et al., 2012). For example, miR-126 up-regulation promotes mesenchymal stem cell (MSC) secretome and ischemic angiogenesis and improves cardiac function (Huang et al., 2013).

FOXO3a is a major downstream effector of phosphatidylinositol 3-kinase (PI3K)/Akt signaling pathway in regulating endothelial cell survival and vascular endothelial function (Tian et al., 2015; Ren et al., 2016; Li and Zheng, 2019; Yao et al., 2019; Huang et al., 2015; Yan et al., 2019). Burns induce inactivation of PI3K/Akt and dephosphorylation of FOXO3a, which translocates into the nucleus and triggers apoptosis-related gene expression (Yu et al., 2016). Several evidences have demonstrated that stem cell transplantation improves cardiac function through the Akt survival pathway in diabetic cardiomyopathy (Yan and Singla, 2013). In addition, IGF-1 released from adipose stem cells protects against 6-hydroxydopamine-induced neurotoxicity/neuronal cell death via PI3K/Akt and downstream signaling pathway (Wang et al., 2014).

Based on the published studies and our previous results, this study was designed to investigate the potential mechanism of the therapeutic effect of hMSC involved in the endothelial apoptosis and dysfunctions of endothelial barrier at early stage post severe burn.

RESULTS

IGF-1 Secreted from hMSC Reduces Severe Burn-Induced Apoptosis of Endothelial Cells

To investigate the role of hMSC-secreted IGF-1 on severe burn-induced apoptosis of endothelial cells, we over-expressed and knocked down IGF-1 in hMSC and assessed human umbilical vein endothelial cell (HUVEC) apoptosis in the severely burned serum culture system. Flow cytometry assay showed that transfection efficiency was comparable in Lenti-overexpress vehicle (mock), Lenti-IGF-1-overexpression (IGF-1-o), Lenti-siRNA vehicle (mock), and Lenti-IGF-1-siRNA (IGF-1-i) groups (Figures 1A and 1B). Compared with the corresponding mock groups, the mRNA expression of IGF-1 in IGF-1-o and IGF-1-i groups was significantly increased or decreased, respectively (Figure 1C). After cultured with or without burn serum, the mRNA, protein, and secreted levels of IGF-1 in burn serum + hMSC group were remarkably higher than those in control and sham serum + hMSC groups. Consistently, the mRNA, protein, and secreted levels of IGF-1 were significantly higher and lower in IGF-1-o and IGF-1-i groups than in the corresponding mock groups, respectively (Figures 1D–1F).

To investigate the paracrine effect of hMSC on severe burn-induced HUVEC apoptosis, hMSC and HUVEC were co-cultured in a trans-well co-culture system, treated with DMEM-high glucose containing 20% severely burned rat serum for 24 h. HUVEC cells were subjected to apoptosis analysis. Apoptosis was boosted in the burn serum group as compared with control and sham serum groups, whereas it was obviously reduced after co-culturing with hMSC (Figure 1G). In addition, IGF-1 overexpression further decreased apoptosis of HUVEC, whereas IGF-1 knockdown increased apoptosis compared with the corresponding mock groups.

MiR-301a-3p Down-Regulation Is Induced by Severe Burn and Acts as a Direct Regulator of IGF-1 in hMSC

To identify dysregulated miRNAs induced by burn in hMSC, miRNA array analysis was performed in hMSCs, which were maintained in a co-culture system of severe burn serum and sham serum (control) for 24 h. The results showed that 31 miRNAs were downregulated and 81 were upregulated (fold change > 2). Among them, miR-301a-3p was the top-ranked downregulated miRNA (Figures 2A and 2B). Reduction of miR-301a-3p induced by burn was also confirmed by real-time PCR assay (Figure 2C). Based on TargetScan and miRanda, we predicted that IGF-1 was a direct target for miR-301a-3p, which was highly conserved across species (Figure 2D). We therefore performed a luciferase assay to evaluate the direct interaction between miR-301a-3p and IGF-1 mRNA. The luciferase activity was inhibited when miR-301a-3p mimics were co-transfected with luciferase reporters containing the predicted binding region of the wild-type 3' UTR of IGF-1 (Figure 2E). However, the luciferase activity remained unchanged when a plasmid with a mutated

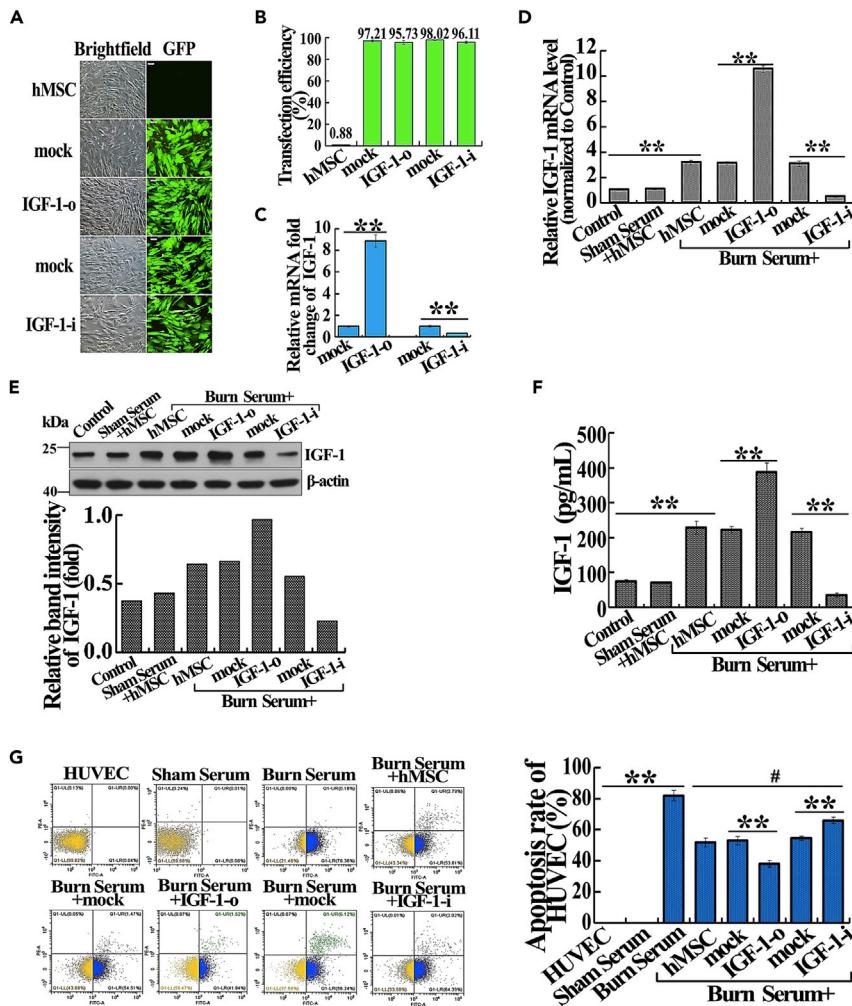


Figure 1. Suppressive Effect of IGF-1 Secreted from hMSC on Severe Burn-Induced HUVEC Apoptosis In Vitro

(A) Representative photographs revealed transfection efficiency with mock, IGF-1-o, mock, IGF-1-i in hMSC (magnification: 100 \times). Visible green fluorescence protein (GFP) expression that >96.77% of the cells were successfully infected.

(B) Transfection efficiencies of mock, IGF-1-o, mock, IGF-1-i groups were evaluated by flow cytometry assay.

(C) The relative mRNA fold change of IGF-1 in hMSC after transfection with mock, IGF-1-o, mock, IGF-1-i were detected by real-time PCR.

(D) The relative mRNA levels of IGF-1 in different treatment groups were detected by real-time PCR.

(E) The protein expression level of IGF-1 in different treatment groups was detected by western blotting.

(F) The IGF-1 level in cultural supernatant of different treatment groups was detected by ELISA assay.

(G) Apoptosis rates of HUVEC in different treatment groups were detected by the flow cytometry assay. The quantitative analyses were presented in the corresponding histogram.

Values are represented as mean \pm SD (n = 6), *p < 0.05, **p < 0.01. The hMSC, mock, IGF-1-o, mock, or IGF-1-i was defined as untransfected, Lenti-overexpression vehicle transfected, Lenti-IGF-1-overexpression transfected, Lenti-siRNA vehicle transfected, and Lenti-IGF-1-siRNA transfected, respectively.

sequence was used instead (Figure 2F). These results suggest that miR-301a-3p is suppressed by burn and directly targets IGF-1.

The miR-301a-3p Regulating hMSC-Secreted IGF-1 Reduces Severe Burn-Induced HUVEC Apoptosis

To determine whether miR-301a-3p modulates severe burn-induced HUVEC apoptosis by regulating hMSC-secreted IGF-1, hMSCs were transfected with Lenti-mimic vehicle (mock), Lenti-miR-301a-3p mimic

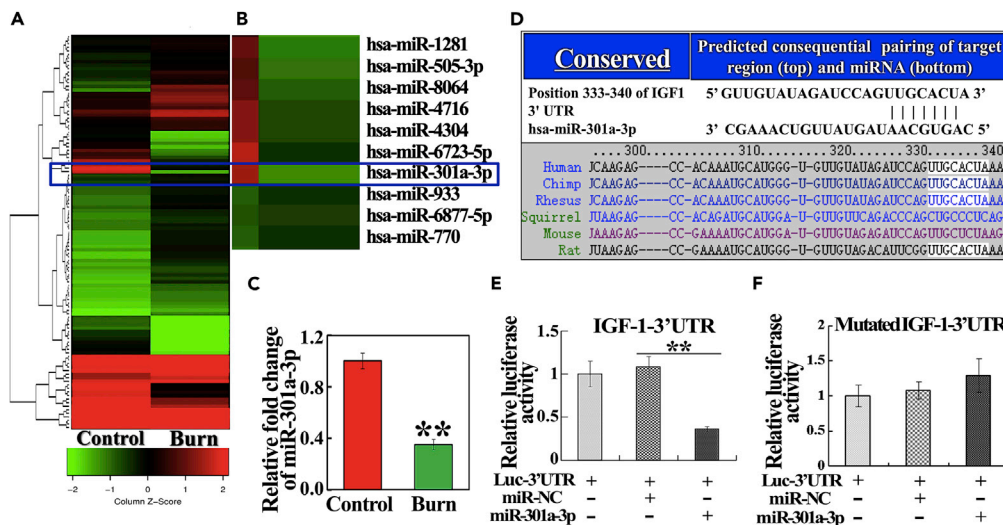


Figure 2. Severe Burn-Induced Down-Regulation of miR-301a-3p Regulated Directly on IGF-1 Protein Translation in hMSC

(A) Hierarchical clustering of miRNAs expressed differentially in hMSC of the control and burn groups. The scale bar at the bottom depicts standard deviation from the mean.
 (B) Enlarged view of miRNAs with significantly differential expression was shown.
 (C) The relative fold change of miR-301a-3p in hMSC of control and burn groups were detected by real-time PCR assay.
 (D) Bioinformatics predicted miR-301a-3p-binding sites in IGF-1. Partial sequences of miR-301a-3p and sequences of its binding sites in the 3' UTR of IGF-1 across various species are shown.
 (E and F) Luciferase activity derived from a reporter containing a wide-type (E) or mutant (F) 3' UTR of IGF-1 co-transfected with miR-301a-3p or miR-NC, respectively. All values are represented as mean \pm SD (n = 3), **p < 0.01.

(miR-301a-3p-o), Lenti-miR-301a-3p mimic combined Lenti-IGF-1-overexpression (miR-301a-3p-o + IGF-1-o), Lenti-inhibitor vehicle (mock), Lenti-miR-301a-3p inhibitor (miR-301a-3p-i), and Lenti-miR-301a-3p inhibitor combined Lenti-IGF-1-siRNA (miR-301a-3p-i + IGF-1-i). The transfection efficiency was comparable among these groups (Figures 3A and 3B). MiR-301a-3p overexpression and inhibition significantly increased and decreased the expression level of miR-301a-3p, respectively (Figure 3C). MiR-301a-3p overexpression obviously repressed the protein expression and secretion of IGF-1. By contrast, downregulation of miR-301a-3p enhanced the protein and secreted abundance of IGF-1 (Figures 3E and 3F). IGF-1 knock-down and overexpression resulted in downregulation and upregulation of IGF-1, respectively (Figures 3D–3F). However, the relative IGF-1 mRNA levels in miR-301a-3p-o and miR-301a-3p-i groups exhibited no significant changes compared with the corresponding mock groups (Figure 3D). These data suggest that miR-301a-3p regulated IGF-1 at the post-transcriptional level.

Next, the hMSC and HUVEC co-culture system was used to evaluate the effect of miR-301a-3p on HUVEC apoptosis induced by burn. Compared with the burn serum group, other groups reduced HUVEC apoptosis rates (Figure 3G). miR-301a-3p overexpression led to enhance HUVEC apoptosis, which was reversed by IGF-1 ectopic expression (Figure 3G). Oppositely, reduction of miR-301a-3p suppressed HUVEC apoptosis, which was reversed by IGF-1 inhibition (Figure 3G). Taken together, down-regulation of miR-301a-3p in hMSC reduces burn-induced HUVEC apoptosis by upregulating IGF-1 expression.

The miR-301a-3p Regulates IGF-1 Levels in Serum and Vital Organs of Severely Burned Rats

To further determine if miR-301a-3p regulates IGF-1 levels *in vivo*, severely burned rats were immediately injected with hMSC, which was co-transfected with IGF-1 and miR-301a-3p. IGF-1 levels in serum and vital organs were detected at 12, 24, and 48 h post severe burn. IGF-1 levels in serum and vital organs, such as lung, liver, kidney, and heart, were decreased in the burn group, whereas they were increased in the burn + hMSC and burn + mock groups, compared with those in the sham group (p < 0.05). Moreover, they were markedly higher in burn + IGF-1-o and burn + miR-301a-3p-i groups and lower in burn + IGF-1-i and burn + miR-301a-3p-o groups than in the burn + mock group (p < 0.05). They were also significantly decreased in miR-301a-3p-i + IGF-1-i groups compared with burn + miR-301a-3p-i groups and were comparable with

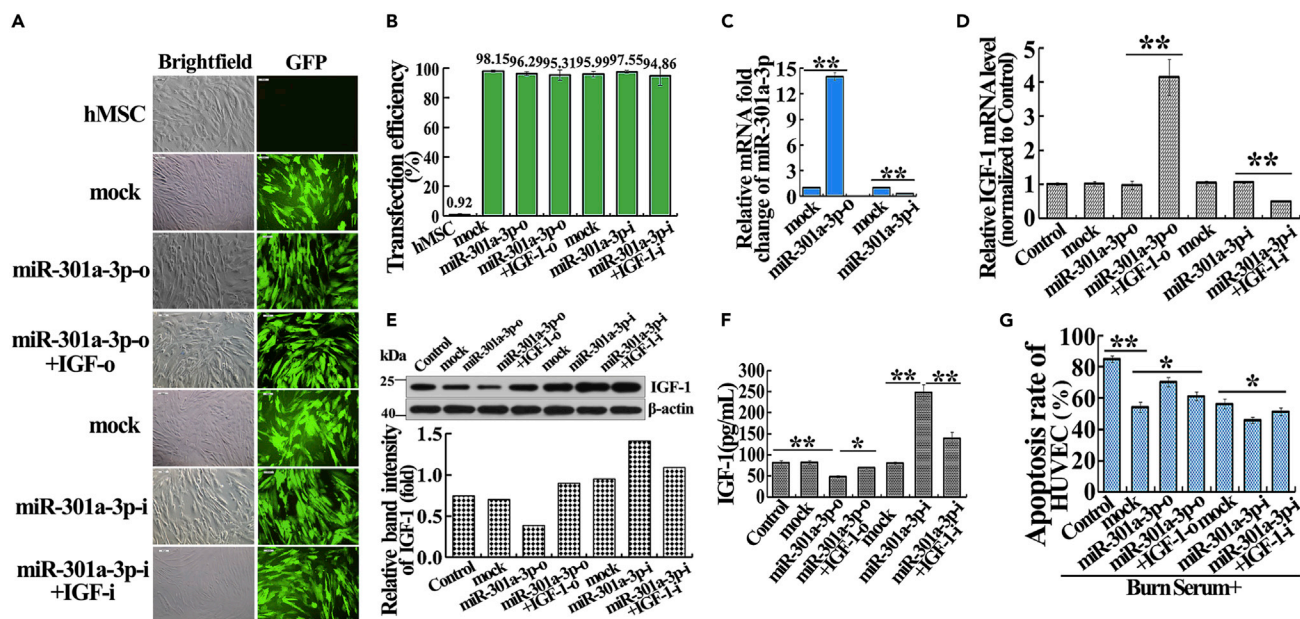


Figure 3. miR-301a-3p Negatively Regulating hMSC-Secreted IGF-1 Reduces Severe Burn-Induced HUVEC Apoptosis In Vitro

(A) Representative photographs demonstrated successful transfection with mock, miR-301a-3p-o, miR-301a-3p-o + IGF-1-o, mock, miR-301a-3p-i, and miR-301a-3p-i + IGF-1-i in hMSC (magnification: 100 \times). Visible green fluorescence protein (GFP) expression that >96.36% of the cells were successfully infected.

(B) Transfection efficiencies of mock, miR-301a-3p-o, miR-301a-3p-o + IGF-1-o, mock, miR-301a-3p-i, and miR-301a-3p-i + IGF-1-i groups were evaluated by flow cytometry assay.

(C) The relative expression levels of miR-301a-3p in hMSC after transfection with mock, miR-301a-3p-o, mock, and miR-301a-3p-i were detected by real-time PCR.

(D) The relative IGF-1 mRNA levels in hMSC of control, mock, miR-301a-3p-o, miR-301a-3p-o + IGF-1-o, mock, miR-301a-3p-i, and miR-301a-3p-i + IGF-1-i groups were detected by real-time PCR.

(E) The relative IGF-1 protein expression levels in hMSC of control, mock, miR-301a-3p-o, miR-301a-3p-o + IGF-1-o, mock, miR-301a-3p-i, and miR-301a-3p-i + IGF-1-i groups were detected by western blotting.

(F) The IGF-1 levels in cultural supernatant of control, mock, miR-301a-3p-o, miR-301a-3p-o + IGF-1-o, mock, miR-301a-3p-i, and miR-301a-3p-i + IGF-1-i groups were detected by ELISA assay.

(G) Apoptosis rates of HUVEC in control, mock, miR-301a-3p-o, miR-301a-3p-o + IGF-1-o, mock, miR-301a-3p-i, and miR-301a-3p-i + IGF-1-i groups were detected by flow cytometry assay in the severely burned serum culture system. The quantitative analyses were presented in the corresponding histogram. Values are represented as mean \pm SD (n = 6), *p < 0.05, **p < 0.01. Control, mock, miR-301a-3p-o, miR-301a-3p-o + IGF-1-o, mock, miR-301a-3p-i, and miR-301a-3p-i + IGF-1-i were defined as untransfected, Lenti-mimics vehicle transfected, Lenti-miR-301a-3p mimics transfected, Lenti-miR-301a-3p mimics and Lenti-IGF-1-overexpress co-transfected, Lenti-inhibitors vehicle transfected, Lenti-miR-301a-3p inhibitors transfected, and Lenti-miR-301a-3p inhibitors and Lenti-IGF-1-siRNA co-transfected, respectively.

burn + mock groups (p < 0.05) (Figures 4A–4F). The results suggest that down-regulation of miR-301a-3p mediates IGF-1 expression and secretion in multiple organs and serum of severely burned rats.

MiR-301a-3p Negatively Regulating hMSC-Secreted IGF-1 Inhibits Vascular Endothelial Apoptosis in Vital Organs in Severely Burned Rats

Based on the above results, we next investigated the effect of miR-301a-3p-mediated IGF-1 secretion from hMSC on vascular endothelial apoptosis of vital organs in severely burned rats. As shown in Figure 5A, the transplanted cells of burn + mock, burn + IGF-1-o, burn + IGF-1-i, burn + miR-301a-3p-o, burn + miR-301a-3p-i, and burn + miR-301a-3p-i + IGF-1-i groups migrated into the lung, liver, kidney, and heart, which were accumulated in the blood vessels of these vital organs at 24 h post severe burn. The vascular endothelial apoptosis of vital organs was not observed in sham groups but was significantly increased in the burn group (p < 0.01) (Figure 5B). hMSC and IGF-1 both obviously suppressed the vascular endothelial apoptosis of vital organs (p < 0.01) (Figures 5B and 5C). Moreover, compared with the burn + mock group, the apoptosis was further decreased in burn + IGF-1-o and burn + miR-301a-3p-i groups but was markedly increased in burn + IGF-1-i and burn + miR-301a-3p-o groups (p < 0.05) (Figures 5B and 5C). The decreased apoptosis in

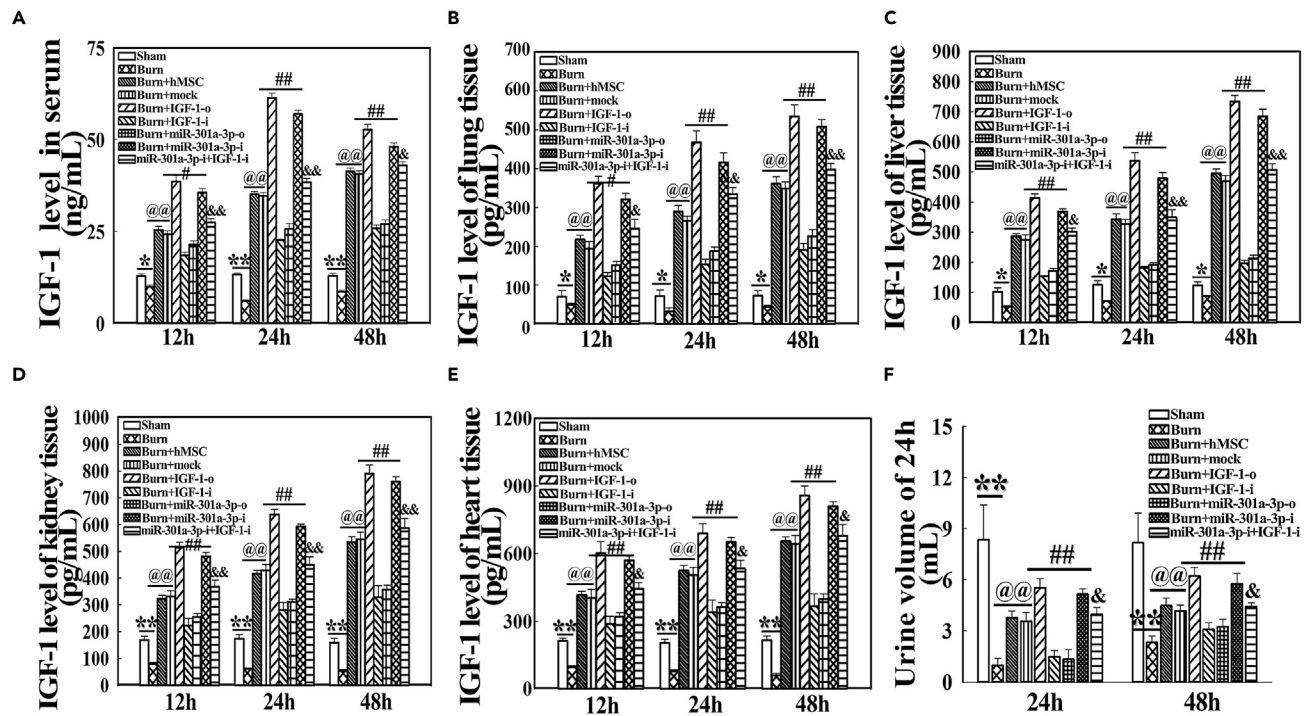


Figure 4. The miR-301a-3p Regulates IGF-1 Levels in Serum and Vital Organs of Severely Burned Rats

(A–E) IGF-1 levels in serum (A) and vital organs, such as lung (B), liver (C), kidney (D), and heart (E), in rats transfected with miR-301a-3p were detected by ELISA assay at 12, 24, and 48 h post severe burn, respectively. The down-regulation expression of miR-301a-3p mediated IGF-1 secretion from the transplanted hMSC in serum and vital organs, such as lung, liver, kidney, and heart, of severely burned rats.

(F) The urine volume was collected and recorded at 24 h post severe burn. Values are represented as mean \pm SD (n = 8). *p < 0.05 and **p < 0.01 compared with sham groups, respectively. @p < 0.05 and @@p < 0.01 compared with burn group, respectively. #p < 0.05 and ##p < 0.01 compared with burn + mock group, respectively. &p < 0.05 and &&p < 0.01 compared with miR-301a-3p-i group, respectively. The mock, IGF-1-o, IGF-1-i, miR-301a-3p-o, miR-301a-3p-i or miR-301a-3p-i + IGF-1-i groups were defined as transplanted hMSC transfected with Lenti-GFP vehicle, Lenti-IGF-1-overexpress, Lenti-IGF-1-siRNA, Lenti-miR-301a-3p mimics and Lenti-miR-301a-3p inhibitors, Lenti-miR-301a-3p inhibitors combined Lenti-IGF-1-siRNA co-transfected, respectively.

burn + miR-301a-3p-i groups was reversed by IGF-1 inhibition (p < 0.05) (Figures 5B and 5C). Collectively, IGF-1 expression directly regulated by miR-301a-3p protects vital organs from burn-induced apoptosis.

MiR-301a-3p Regulating hMSC-Secreted IGF-1 Reduces Vascular Permeability of Vital Organs in Severely Burned Rats

Then we evaluated the therapeutic effect of miR-301a-3p-mediated IGF-1 secretion from hMSC on vascular permeability of vital organs, including lung, liver, kidney, and heart in rats at 12, 24, and 48 h post severe burn by detecting water content ratio and Evans Blue (EB) content. The water content ratios and the EB content of lung, liver, kidney, and heart were increased in the burn group but were decreased in the burn + hMSC group compared with the sham group (p < 0.05). IGF-1 up-regulation and miR-301a-3p down-regulation suppressed the water content ratio and the EB content. Opposite results were observed in IGF-1 inhibition and miR-301a-3p overexpression groups (p < 0.05). IGF-1 down-regulation enhanced the inhibition effect of miR-301a-3p inhibitors on water content ratio and the EB content (Tables 1 and 2).

MiR-301a-3p Negative Regulating hMSC-Secreted IGF-1 Improves the Function Parameters of Vital Organs in Severely Burned Rats

We also evaluated the therapeutic effects of miR-301a-3p-mediated IGF-1 secretion from hMSC on function parameters of lung, liver, kidney, and heart in rats at 24 h post severe burn. Lung function was determined by examining the parameters of inspiratory resistance (Ri), expiratory resistance (Re), compliance (Cl), peak expiratory flow (PEF), and maximal voluntary ventilation (MVV). Liver function was checked by measuring Alanine Transaminase (ALT) and Aspartate Transaminase (AST). Kidney function was determined by detecting urine volume, creatinine (Crea), and Urea. Heart function was determined by measuring

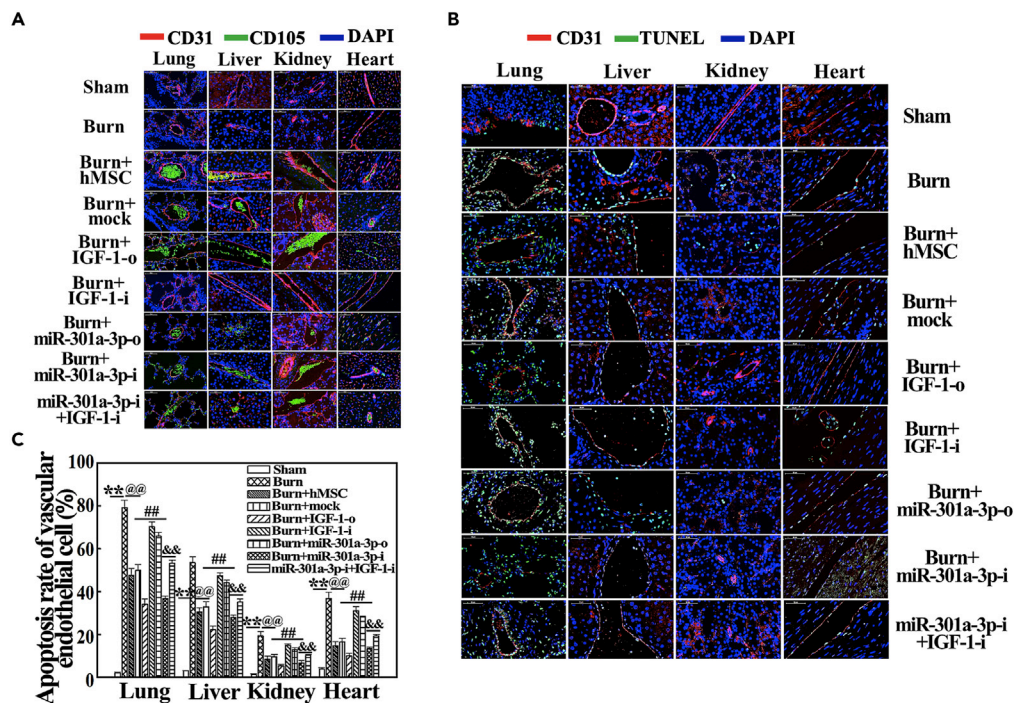


Figure 5. Distribution of Transplanted hMSC with IGF-1/miR-301a-3p Overexpression and Knockdown and Their Effects on Apoptosis of Vascular Endothelial Cell in Vital Organs of Rats at 24 h Post Severe Burn

(A) Representative photographs showed that hMSC transfected with mock, IGF-1-o, IGF-1-i, miR-301a-3p-o, miR-301a-3p-i, and miR-301a-3p-i + IGF-1-i were mainly distributed in blood vessels of lung, liver, kidney, and heart tissues in rats at 24 h post severe burn.

(B) miR-301a-3p negatively regulating hMSC-secreted IGF-1 reduced vascular endothelial apoptosis of vital organs, such as lung, liver, kidney, and heart, in severely burned rats at 24 h post injury.

(C) Quantitative analysis of apoptosis rate is shown in the corresponding histogram. Values are represented as mean \pm SD (n = 8). *p < 0.05 and **p < 0.01 compared with sham group, respectively. @p < 0.05 and @@p < 0.01 compared with burn group, respectively. #p < 0.05 and ##p < 0.01 compared with burn + mock group, respectively. &p < 0.05 and &&p < 0.01 compared with miR-301a-3p-i group, respectively.

Troponin, Creatine Kinase (CK), MB isoform of CK (CK-MB), and Lactate Dehydrogenase (LDH) and a-hydroxybutyrate Dehydrogenase (HBDH). We showed that the multiple organ functions were deteriorated in the burn group but significantly improved in the burn + hMSC group compared with the sham group (p < 0.05). Compared with the burn + mock group, they were greatly improved in burn + IGF-1-o and burn + miR-301a-3p-i groups and markedly deteriorated in burn + IGF-1-i and burn + miR-301a-3p-o groups (p < 0.05). Moreover, compared with the burn + miR-301a-3p-i group, these parameters were worsened again in the miR-301a-3p-i + IGF-1-i group, and close to burn + mock group (Table 3) (p < 0.05). Taken together, these data comprehensively confirmed the therapeutic effects of miR-301a-3p-mediated IGF-1 secretion on vascular endothelial apoptosis, vascular permeability, and function parameters of vital organs, such as lung, liver, kidney, and heart in rats at very early stages post severe burn.

miR-301a-3p Negatively Regulates hMSC-Secreted IGF-1 to Activate PI3K/Akt/FOXO3 Signal in Endothelial Cells

To elucidate the potential mechanism, we examined PI3K/Akt signaling using western blotting. The phosphorylation of PI3K, AKT, and Foxo3a was normalized to their protein expression. Cleaved caspase 3 was normalized to caspase 3. Compared with control and sham serum groups, the p-PI3K/PI3K, p-Akt/Akt, and p-FOXO3a/FOXO3a were decreased in the burn serum group but increased in IGF-1-treated groups in a dose-dependent manner (Figure 6A) (p < 0.05). In addition, the p-PI3K/PI3K, p-Akt/Akt, and p-FOXO3a/FOXO3a of the burn serum group were lower than in the sham serum group, and those of the burn + mock group were markedly higher than in the burn group, but markedly lower than in the sham serum group (p < 0.05). They were remarkably increased in burn + IGF-1-o and burn + miR-301a-3p-i groups,

Groups	Parameter											
	Lung			Liver			Kidney			Heart		
	12 h	24 h	48 h	12 h	24 h	48 h	12 h	24 h	48 h	12h	24 h	48 h
Sham	63.15 ± 1.54	64.46 ± 0.77	63.94 ± 1.68	70.01 ± 1.54	71.16 ± 1.34	70.74 ± 1.38	78.48 ± 1.02	77.25 ± 2.74	78.58 ± 1.20	60.85 ± 1.39	61.18 ± 0.96	60.98 ± 1.02
Burn	90.19 ± 1.39 **	96.57 ± 2.08 **	85.92 ± 1.14 **	92.07 ± 0.62 **	97.24 ± 1.51 **	86.02 ± 2.03 **	85.19 ± 0.98**	90.58 ± 1.63 **	82.72 ± 2.69	81.46 ± 1.64 **	85.36 ± 2.16**	76.45 ± 1.11 **
Burn + hMSC	76.24 ± 0.88 @@	80.3 ± 1.15 @@	73.09 ± 1.20 @@	82.95 ± 1.03 @@	84.87 ± 1.29 @@	78.81 ± 1.38 @@	80.19 ± 0.71 @@	83.44 ± 0.95 @@	78.72 ± 1.90	70.05 ± 1.12 @@	74.80 ± 1.09@@	68.38 ± 1.06 @@
Burn + mock	76.97 ± 0.51 @@	81.24 ± 1.04 @@	74.71 ± 2.45 @@	83.39 ± 0.88 @@	85.95 ± 0.97 @@	78.15 ± 1.20 @@	80.50 ± 1.13 @@	83.73 ± 0.78 @@	78.53 ± 1.47	70.96 ± 0.63 @@	74.99 ± 0.54 @@	68.85 ± 0.71 @@
Burn + IGF-o	68.24 ± 1.49 ##	72.36 ± 1.81 #	67.07 ± 1.07 ##	76.15 ± 1.03 ##	78.01 ± 1.06 ##	74.09 ± 0.74 #	78.12 ± 0.85	79.51 ± 0.96 #	78.37 ± 0.96	65.49 ± 0.41 #	67.66 ± 0.90 ##	64.12 ± 0.55 #
Burn + IGF-i	86.03 ± 0.76 ##	91.97 ± 0.74 ##	81.99 ± 0.88 ##	89.05 ± 0.56 ##	93.00 ± 1.35 ##	83.98 ± 0.97 #	83.22 ± 0.78	88.73 ± 0.54 #	81.93 ± 1.50	78.90 ± 0.84 ##	82.82 ± 0.45 ##	73.07 ± 1.44 #
Burn + miR-301a-3p-o	84.12 ± 0.85 ##	88.86 ± 1.31 ##	79.24 ± 0.92 #	87.29 ± 1.04 #	91.81 ± 0.77 ##	82.57 ± 2.16	82.86 ± 0.49	87.24 ± 1.06 #	80.64 ± 3.35	77.13 ± 0.72 ##	80.79 ± 0.58 ##	72.88 ± 1.57
Burn + miR-301a-3p-i	70.28 ± 0.83 #	74.27 ± 0.59 ##	69.33 ± 1.20 #	77.48 ± 0.90 ##	80.35 ± 0.59 #	75.64 ± 1.11	79.46 ± 0.81	80.02 ± 0.49 #	79.11 ± 0.72	66.98 ± 0.55 #	69.04 ± 0.86 ##	65.03 ± 0.98 #
miR-301a3p-i +IGF-1-i	75.52 ± 1.12 &	79.91 ± 0.84 &	72.94 ± 1.05 &	81.93 ± 0.74 &	84.36 ± 0.78 &	77.83 ± 1.00	81.3 ± 0.92	83.08 ± 0.72 &	79.48 ± 0.82	69.77 ± 0.79 &	72.85 ± 0.92 &	67.14 ± 0.56

Table 1. Water Content Ratio of Vital Organs (mean ± SD, %, n = 8)

miR-301a-3p negatively regulating hMSC-secreted IGF-1 reduces water content ratio of vital organs in severely burned rats (mean ± SD, n = 8). *p < 0.05 and **p < 0.01 compared with sham group, respectively. @p < 0.05 and @@p < 0.01 compared with burn group, respectively. #p < 0.05 and ##p < 0.01 compared with burn + mock group, respectively. &p < 0.05 and &&p < 0.01 compared with burn + miR-301a-3p-i group, respectively.

but obviously decreased in burn + IGF-1-i and burn + miR-301a-3p-o groups compared with burn + mock group (p < 0.05). Moreover, IGF-1 inhibition suppressed the expression of p-PI3K/PI3K, p-Akt/Akt, and p-FOXO3a/FOXO3a (Figure 6B) (p < 0.05). By contrast, the ratio of cleaved Caspase 3 to Caspase 3 showed opposite change tendency relative to p-PI3K/PI3K, p-Akt/Akt, and p-FOXO3a/FOXO3a (Figures 6A and 6B). The data confirmed that miR-301a-3p regulation of hMSC-secreted IGF-1 activated PI3K/Akt/FOXO3a signal of vascular endothelial cells in severe burn microenvironment *in vitro*.

DISCUSSION

Burn is a common form of traumatic injury with high mortality and morbidity. The vascular endothelium injury leading to vascular endothelial barrier dysfunction, which is essential for the initiation of shock at the early stage and progression of multiple organ dysfunction at the advanced stage. Recently, the therapeutic effects of hMSC have been demonstrated on some severe traumas and serious injuries through stabilizing endothelial barrier function (Walker et al., 2010; Bruno et al., 2012; Gatti et al., 2011; Walter et al., 2014; Yang et al., 2015; Meng et al., 2019). We previously found that hMSC alleviated cells apoptosis of wound and organ tissues post severe burn by secreting bioactive factors (Liu et al., 2016; Bake et al., 2019). In this study, we found that hMSC significantly reduced severe burn-induced vascular endothelial

Groups	Parameter											
	Lung			Liver			Kidney			Heart		
	12 h	24 h	48 h	12 h	24 h	48 h	12 h	24 h	48 h	12 h	24 h	48 h
Sham	10.87 ± 0.93	11.26 ± 0.82	10.95 ± 1.16	11.81 ± 0.66	11.23 ± 0.22	10.93 ± 0.50	10.52 ± 0.81	10.11 ± 0.26	10.00 ± 0.79	14.14 ± 0.85	14.18 ± 1.02	13.78 ± 1.01
Burn	56.55 ± 2.80**	62.18 ± 3.33**	40.74 ± 0.95**	32.63 ± 0.58**	40.60 ± 0.35**	25.92 ± 1.09**	23.48 ± 1.05**	35.56 ± 1.04**	18.61 ± 0.83**	27.81 ± 1.00**	38.23 ± 2.05**	20.92 ± 0.56*
Burn + hMSC	28.96 ± 0.92@@	37.69 ± 1.85@@	21.80 ± 1.09@@	19.90 ± 0.73@@	23.77 ± 0.94@@	16.48 ± 1.20@@	16.01 ± 0.48@@	21.79 ± 1.04@@	13.50 ± 0.62@	18.52 ± 1.13@@	22.70 ± 1.10@@	15.54 ± 1.02@
Burn + mock	29.03 ± 1.01@@	38.51 ± 2.49@@	22.93 ± 0.61@@	20.36 ± 0.85@@	24.05 ± 0.68@@	16.96 ± 0.85@@	16.24 ± 0.77@@	22.33 ± 0.50@@	13.92 ± 1.14@	19.04 ± 0.95@@	23.08 ± 0.94@@	15.69 ± 0.95@
Burn + IGF-o	19.85 ± 1.35##	23.06 ± 1.70##	14.44 ± 0.70##	13.93 ± 0.57##	15.46 ± 0.41##	12.65 ± 0.76#	12.71 ± 0.54#	15.54 ± 0.89#	10.87 ± 1.03#	14.60 ± 0.47#	16.52 ± 0.78##	14.05 ± 1.19
Burn + IGF-i	47.96 ± 2.96##	55.58 ± 1.36##	35.59 ± 0.88##	27.80 ± 0.72##	35.79 ± 0.90##	21.80 ± 0.88#	20.76 ± 0.32#	31.73 ± 0.92##	16.35 ± 1.50#	25.01 ± 0.92#	35.05 ± 0.60##	19.04 ± 0.87#
Burn + miR-301a-3p-o	45.78 ± 1.04##	52.70 ± 1.81##	33.37 ± 1.04##	25.94 ± 1.19#	32.81 ± 1.42##	20.97 ± 1.30#	19.81 ± 0.20#	29.11 ± 0.18#	15.89 ± 0.77#	23.99 ± 0.73#	33.73 ± 1.39##	18.97 ± 1.03#
Burn + miR-301a-3p-i	22.06 ± 0.67##	25.93 ± 0.62##	16.80 ± 0.65##	15.20 ± 0.71#	17.18 ± 0.85##	13.08 ± 1.12#	13.29 ± 1.40#	17.02 ± 0.75#	11.43 ± 0.99#	15.50 ± 1.09#	17.42 ± 0.71##	15.12 ± 0.91
miR-301a3p-i + IGF-1-i	26.55 ± 1.14&	33.79 ± 1.26&&	19.82 ± 0.70&	18.71 ± 1.08&	21.89 ± 1.21&	15.24 ± 0.93	14.89 ± 0.50	20.14 ± 0.37&	13.79 ± 0.51	17.38 ± 1.25	21.35 ± 1.12&	16.33 ± 1.79

Table 2. Evans Blue Content in Supernatant of Vital Organs (mean ± SD, µg/mL, n = 8)

MiR-301a-3p negatively regulating hMSC-secreted IGF-1 reduces Evans blue content in supernatant of vital organs in severely burned rats (mean ± SD, n = 8). *p < 0.05 and **p < 0.01 compared with sham group, respectively. @p < 0.05 and @@p < 0.01 compared with burn group, respectively. #p < 0.05 and ##p < 0.01 compared with burn + mock group, respectively. &p < 0.05 and &&p < 0.01 compared with burn + miR-301a-3p-i group, respectively.

apoptosis, protected against endothelial barrier disorder and multiple organ dysfunction by secreting IGF-1. Severe burn-induced down-regulation of miR-301a-3p directly increased IGF-1 synthesis and secretion in hMSC, hence reducing vascular endothelial apoptosis and protecting against dysfunction of endothelial barrier and multiple organs. We also demonstrated that miR-301a-3p negatively regulated hMSC-secreted IGF-1 to activate PI3K/Akt/FOXO3 signaling in endothelial cells. Overall, we clarified the potential mechanism of hMSC on the endothelial apoptosis and dysfunctions of endothelial barrier at early stage post severe burn.

As a key mitogenic and anti-apoptosis factor, IGF-1 exhibits pro-survival and repairing effect on endothelial barrier, which is susceptible to ectopic expression and dysfunction induced by excessive inflammation, serious metabolic disturbance, and other systematic disorders after severe burn or trauma (Aman et al., 2016; Bake et al., 2019; Davis et al., 2006). Our precious study showed that IGF-1 was a pivotal bioactive factor secreted by hMSC in alleviating cell apoptosis after severe burn (Liu et al., 2014). Here we demonstrated that IGF-1 secreted by hMSC displayed a strong anti-apoptotic activity and therapeutic effects. IGF-1 reduced severe burn-induced vascular endothelial apoptosis, protected against endothelial barrier disorder, and multiple organ dysfunction *in vitro* and *in vivo*. It has been shown that bone marrow-derived MSC has beneficial effects on tubular cell repair in acute kidney injury by producing IGF-1 (Imberti et al.,

Groups	Parameter													
	Lung Function					Liver Function		Kidney Function		Heart Function				
	Inspiratory Resistance (R _i , cm H ₂ O/mL.s)	Expiratory Resistance (R _e , cm H ₂ O/mL.s)	Compliance (Cl, mL/cm H ₂ O)	The Peak Expiratory Flow (PEF, mL/min)	Maximal Voluntary Ventilation (MVV, mL)	ALT (U/L)	AST (U/L)	Urea (mmol/L)	Crea (mmol/L)	Troponin (pg/mL)	CK (U/L)	CK-MB (U/L)	LDH (U/L)	HBDH (U/L)
Sham	1.80 ± 0.09	1.37 ± 0.05	0.28 ± 0.02	38.09 ± 1.67	194.46 ± 3.27	39.51 ± 3.73	133.49 ± 32.18	4.55 ± 0.64	16.5 ± 0.71	210.24 ± 11.57	1,439.5 ± 140.12	1,520.5 ± 186.34	1,402 ± 138.63	469.50 ± 60.93
Burn	5.45 ± 0.13**	4.48 ± 0.09**	0.11 ± 0.03*	20.24 ± 2.04**	121.07 ± 2.38**	210.33 ± 8.57**	892.41 ± 56.33**	13.63 ± 0.71**	27.48 ± 0.63**	320.78 ± 15.35**	5,741.26 ± 137.51**	3,620.97 ± 91.29**	3,431.17 ± 165.74**	1,183.82 ± 166.27**
Burn + hMSC	3.31 ± 0.40@@	2.70 ± 0.38@@	0.20 ± 0.02@	31.72 ± 1.15@@	163.96 ± 1.85@@	113.10 ± 4.18@@	542.39 ± 20.05@@	8.59 ± 0.50@@	22.18 ± 0.77@	259.39 ± 8.70@@	2,952.80 ± 73.15@@	2,490.38 ± 56.64@@	2,172.86 ± 72.10@@	721.95 ± 38.17@@
Burn + mock	3.54 ± 0.18@@	2.99 ± 0.17@@	0.20 ± 0.04	31.38 ± 0.93@@	163.81 ± 2.04@@	114.67 ± 9.36@@	544.85 ± 34.41@@	8.76 ± 0.88@@	22.96 ± 0.49@	261.46 ± 9.98@@	2,967.96 ± 62.97@@	2,518.10 ± 90.01@@	2,221.33 ± 85.71@@	742.92 ± 41.24@@
Burn + IGF-o	2.19 ± 0.17#	1.84 ± 0.56#	0.26 ± 0.02	36.49 ± 0.68#	182.75 ± 3.66##	68.72 ± 6.35##	357.33 ± 28.80##	5.94 ± 0.27##	18.01 ± 0.36#	229.32 ± 10.27#	2054.76 ± 90.29##	1903.48 ± 103.4##	1,696.57 ± 68.84##	585.71 ± 18.48##
Burn + IGF-i	4.73 ± 0.20##	4.17 ± 0.38##	0.13 ± 0.05	23.57 ± 0.51#	132.07 ± 2.03##	187.27 ± 9.59##	825.48 ± 36.10##	11.09 ± 0.45#	25.51 ± 0.14#	294.21 ± 13.52#	4,562.19 ± 115.26##	3,360.51 ± 57.32##	3,074.95 ± 109.12##	1,003.92 ± 42.77##
Burn + miR-301a-3p-o	4.28 ± 0.11##	3.86 ± 0.20##	0.14 ± 0.03	24.49 ± 1.25#	136.71 ± 3.12##	178.68 ± 7.44##	784.52 ± 20.45##	10.54 ± 0.62#	24.82 ± 0.53#	289.65 ± 3.26#	4,357.34 ± 197.05##	3,283.94 ± 45.15##	2,918.33 ± 70.31##	984 ± 25.91##
Burn + miR-301a-3p-i	2.55 ± 0.16#	2.05 ± 0.23#	0.25 ± 0.04	35.72 ± 1.03	179.96 ± 1.94##	75.35 ± 3.82##	371.19 ± 26.71##	6.34 ± 0.19##	19.15 ± 0.79#	234.05 ± 9.51#	2,211.38 ± 79.67##	2075.37 ± 42.71##	1743.22 ± 91.29##	610.11 ± 20.10##
miR-301a3p-i +IGF-1-i	3.09 ± 0.25&	2.52 ± 0.24&	0.22 ± 0.03	32.02 ± 1.09&	167.24 ± 1.51&	100.72 ± 13.59&&	481.48 ± 29.28&&	7.94 ± 0.52&	21.95 ± 0.54&	250.29 ± 4.03&	2,708.84 ± 35.44&&	2,326.95 ± 76.74&	2075.02 ± 79.63&&	697.73 ± 26.38&

Table 3. Function Parameters of Vital Organs (mean ± SD, n = 8)

MiR-301a-3p negatively regulating hMSC-secreted IGF-1 improves function parameters of vital organs in severely burned rats (mean ± SD, n = 8). ALT, alanine transaminase; AST, aspartate transaminase, Crea, creatinine; CK, creatine kinase; CK-MB, MB isoform of CK; LDH, lactate dehydrogenase; HBDH, a-hydroxybutyrate dehydrogenase. *p < 0.05 and **p < 0.01 compared with sham group, respectively. @p < 0.05 and @@p < 0.01 compared with burn group, respectively. #p < 0.05 and ##p < 0.01 compared with burn + mock group, respectively. &p < 0.05 and &&p < 0.01 compared with burn + miR-301a-3p-i group, respectively.

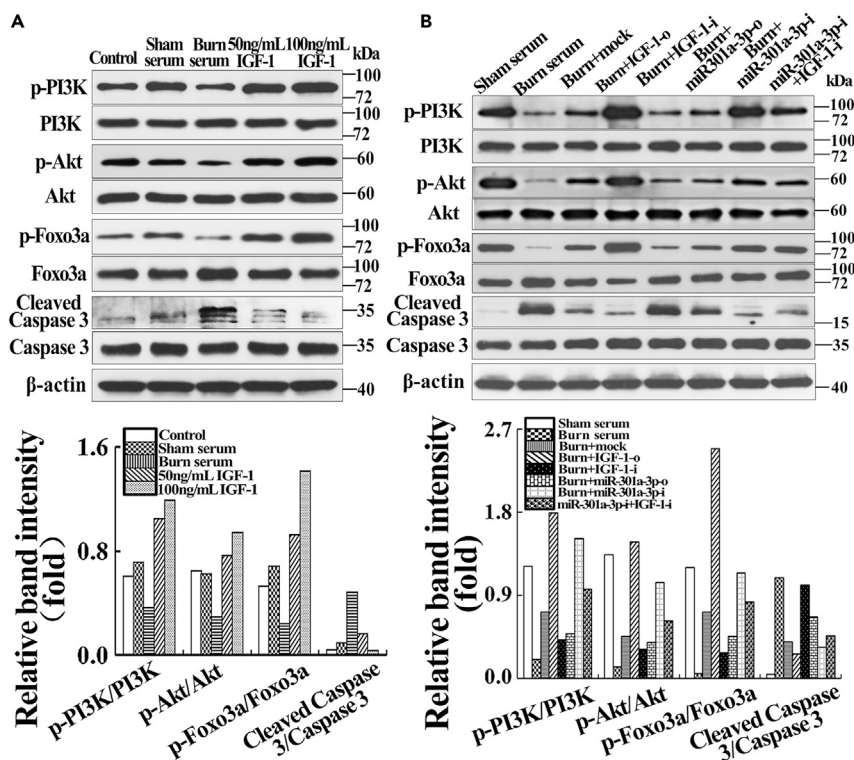


Figure 6. Effects of IGF-1 and hMSC Transfected with IGF-1/miR-301a-3p Overexpression and Knockdown on PI3K/Akt/FOXO3a Signaling of Endothelial Cells in Severely Burned Serum Culture System

(A) Severe burn impaired activation of PI3K/Akt and its downstream effector FOXO3a, and IGF-1 activated PI3K/Akt/FOXO3a in a dose-dependent manner. The quantitative analysis was reported in the corresponding histogram.

(B) MiR-301a-3p negatively regulated hMSC-secreted IGF-1 inhibited PI3K/Akt/FOXO3a signaling of endothelial cells in the severely burned serum culture system; three samples in each group were applied for analysis. The quantitative analysis was reported in the corresponding histogram.

2007). In rats with myocardial infarction, human cardiac stem cells with IGF-1 overexpression enhanced myocardial repair by improving the long-term survival of transplanted cells and the surrounding myocardium (Jackson et al., 2015). Therefore, based on this, IGF-1 secreted by the transplanted hMSC not only protects against apoptosis of the vascular endothelial and dysfunction of endothelial barrier but also exerts a self-protection function in the organic microenvironment post severe burn.

Increasing evidences have reported that MSC exerts their beneficial influences on repair and regeneration of injured organs through miRNA-mediated bioactive factors production and secretion (Lakshmiathy and Hart, 2008; Wen et al., 2012). We herein attempted to profile the microRNAs induced by burn to regulate hMSC-secreted IGF-1. We found that severe burn induced the down-regulation of miR-301a-3p. IGF-1 was a direct target for miR-301a-3p. In fact, miR-301a-3p negatively regulated IGF-1 protein translation and secretion in hMSC. Inhibition of miR-301a-3p in hMSC reduced the apoptosis of HUVECs *in vitro* as well as the apoptosis of vascular endothelial cells *in vivo*, thereby promoting the endothelial barrier permeability of lung, liver, kidney, and heart and eventually improving the function parameters of these organs in severely burned rats. Therefore, this study provided strong evidences supporting that miR-301a-3p directly regulated the production of IGF-1 from hMSC, which functions as a key upstream repair mechanism of hMSC's therapeutic effect on stabilizing endothelial barrier function. Antagonizing miR-301a-3p is a promising strategy to enhance IGF-1 release, which may be a helpful therapy for dysfunction of endothelial barrier and multiple organs. Meanwhile, our team profiled the dysregulated miRNAs after severe burn and its relationship with the biological characteristics of hMSC, which could augment the opportunities to safely pursue better therapeutic modalities during MSC-based therapy in severely burned patients who develop multiple organ dysfunction, even failure.

Finally, we clarified the anti-apoptosis mechanism of IGF-1 secreted by hMSC, which is the downstream signaling of hMSC on protecting against vascular endothelial apoptosis and endothelial barrier dysfunction. PI3K/Akt/FoxO3a signaling participates in regulating cell survival after severe burns. We also showed that severe burn impaired PI3K/Akt activation and increased total FOXO3a protein and cleaved caspase 3 levels, subsequently resulting in apoptosis of vascular endothelial cells. IGF-1 activated PI3K/Akt signaling, increased p-FOXO3a/FOXO3a level, and decreased cleaved Caspase 3/Caspase 3 level. Furthermore, we found that hMSC with IGF-1 overexpression and miR-301a-3p inhibitors remarkably increased PI3K and Akt phosphorylation and the ratio of p-FOXO3a to FOXO3a and decreased the ratio of cleaved Caspase 3 to Caspase 3. On the contrary, hMSC with IGF-1 siRNA and miR-301a-3p mimics could remarkably decrease PI3K and Akt phosphorylation and the ratio of p-FOXO3a/FOXO3a and increase the ratio of cleaved Caspase 3 to Caspase 3. These data confirmed miR-301a-3p negatively regulating hMSC-secreted IGF-1 reduced severe burn-induced vascular endothelial apoptosis via activating PI3K/Akt/FOXO3a signaling. And studies showed that phosphorylation of FOXOs by Akt inhibited transcriptional functions of FOXOs and contributed to cell survival, growth, and proliferation, thereby protecting against injured tissue or organ function (Zhang et al., 2011, 2019; Tucka et al., 2014). In addition, FOXO3 was also considered an evolutionarily conserved longevity factor, and FOXO3-activated vascular cells exhibited delayed aging and increased resistance to injury, even FOXO3-enhanced vascular cells could promote vascular regeneration in a mouse model of ischemic injury (Flachsbart et al., 2017; Martins et al., 2016; Yan et al., 2019).

Conclusion

In summary, these comprehensive data suggested that down-regulation of miR-301a-3p directly regulated hMSC-secreted IGF-1 to reduce severe burn-induced vascular endothelial apoptosis and protected against dysfunction of endothelial barrier and multiple organs via activating PI3K/Akt/FOXO3a signaling. Moreover, our results not only confirmed the potential mechanism involved in the therapeutic effect of hMSC on the endothelial apoptosis and dysfunctions of endothelial barrier at the early stage post severe burn but also might provide the theoretical foundation for further clinical applications of hMSC application into burn areas.

Limitations of the Study

Our study demonstrated the functional role of miR-301a-3p that directly regulated hMSC-secreted IGF-1 to protect against dysfunction of multiple organs *in vivo* and *in vitro*. Although we found the therapeutic effect of hMSC through downregulation of miR-301a-3p expression, the precise role of PI3K/Akt/FOXO3a signaling in mediating the therapeutic effect of hMSC needs further study.

Resource Availability

Lead Contact

Further information and requests for resources and reagents will be provided by the Lead Contact, Jiake Chai (cj304@126.com).

Materials Availability

This study did not involve any new unique reagents or resources.

Data and Code Availability

All data are included in the published article and the [Supplemental Information](#), and any additional information will be available from the lead contact upon request.

METHODS

All methods can be found in the accompanying [Transparent Methods supplemental file](#).

SUPPLEMENTAL INFORMATION

Supplemental Information can be found online at <https://doi.org/10.1016/j.isci.2020.101383>.

ACKNOWLEDGMENTS

This work was supported by research projects of National Natural Science Foundation of China (81701900, 81571894, 81772067), Nursery Fund of PLA General Hospital (17KMM28), the First Affiliated Hospital to the

PLA General Hospital Science Research Foundation (2017FC-304M-CXY-01) and Translational Medicine Foundation of PLA General Hospital (2017TM-029) and Major Project of Military Logistical Support Department (AWS15J003 and ALB19J001).

AUTHOR CONTRIBUTIONS

L.L., H.Y., X.H., H.S.: conception and design, collection and assembly of data, data analysis and interpretation, and manuscript writing; J.C.: conception and design, financial support, data interpretation, and final approval of the manuscript; H.D., Y. Chang, L.Y., Y.W., S.H., X.W., X.Y., Y. Chi, W.L., Q.W., H.W., H.B., X.S., S.L.: provision of study material, data analysis, and interpretation.

DECLARATION OF INTERESTS

The authors declare that they have no competing interests.

Received: October 8, 2019

Revised: June 5, 2020

Accepted: July 15, 2020

Published: August 21, 2020

REFERENCES

- Aman, J., Weijers, E.M., van Nieuw Amerongen, G.P., Malik, A.B., and van Hinsbergh, V.W. (2016). Using cultured endothelial cells to study endothelial barrier dysfunction: challenges and opportunities. *Am. J. Physiol. Lung Cell Mol Physiol.* *311*, L453–L466.
- Auger, C., Samadi, O., and Jeschke, M.G. (2017). The biochemical alterations underlying post-burn hypermetabolism. *Biochim. Biophys. Acta Mol. Basis Dis.* *1863*, 2633–2644.
- Bake, S., Okoreeh, A., Khosravian, H., and Sohrabji, F. (2019). Insulin-like Growth Factor (IGF)-1 treatment stabilizes the microvascular cytoskeleton under ischemic conditions. *Exp. Neurol.* *311*, 162–172.
- Beltran, S.R., Svoboda, K.K., Kerns, D.G., Sheth, A., and Prockop, D.J. (2015). Anti-inflammatory protein tumor necrosis factor- α -stimulated protein 6 (TSG-6) promotes early gingival wound healing: an in vivo study. *J. Periodontol.* *86*, 62–71.
- Bruno, S., Grange, C., Collino, F., Deregibus, M.C., Cantaluppi, V., Biancone, L., Tetta, C., and Camussi, G. (2012). Microvesicles derived from mesenchymal stem cells enhance survival in a lethal model of acute kidney injury. *PLoS One* *7*, e33115.
- Davis, M.E., Hsieh, P.C., Takahashi, T., Song, Q., Zhang, S., Kamm, R.D., Grodzinsky, A.J., Anversa, P., and Lee, R.T. (2006). Local myocardial insulin-like growth factor 1 (IGF-1) delivery with biotinylated peptide nanofibers improves cell therapy for myocardial infarction. *Proc. Natl. Acad. Sci. U S A* *103*, 8155–8160.
- Dorronsoro, A., and Robbins, P.D. (2013). Regenerating the injured kidney with human umbilical cord mesenchymal stem cell-derived exosomes. *Stem Cell Res Ther.* *4*, 39.
- Flachsbart, F., Dose, J., Gentschew, L., Geismann, C., Caliebe, A., Knecht, C., Nygaard, M., Badarinarayan, N., Elsharawy, A., May, S., et al. (2017). Identification and characterization of two functional variants in the human longevity gene FOXO3. *Nat. Commun.* *8*, 2063.
- Gatti, S., Bruno, S., Deregibus, M.C., Sordi, A., Cantaluppi, V., Tetta, C., and Camussi, G. (2011). Microvesicles derived from human adult mesenchymal stem cells protect against ischaemia-reperfusion-induced acute and chronic kidney injury. *Nephrol. Dial. Transpl.* *26*, 1474–1483.
- Haines, R.J., Wang, C.Y., Yang, C.G.Y., Eitner, R.A., Wang, F., and Wu, M.H. (2017). Targeting palmitoyl acyltransferase ZDHHC21 improves gut epithelial barrier dysfunction resulting from burn-induced systemic inflammation. *Am. J. Physiol. Gastrointest. Liver Physiol.* *313*, G549–G557.
- Huang, F., Zhu, X., Hu, X.Q., Fang, Z.F., Tang, L., Lu, X.L., and Zhou, S.H. (2013). Mesenchymal stem cells modified with miR-126 release angiogenic factors and activate Notch ligand Delta-like-4, enhancing ischemic angiogenesis and cell survival. *Int. J. Mol. Med.* *31*, 484–492.
- Huang, L., Wang, F., Wang, Y., Cao, Q., Sang, T., Liu, F., and Chen, S. (2015). Acidic fibroblast growth factor promotes endothelial progenitor cells function via Akt/FOXO3a pathway. *PLoS One* *10*, e0129665.
- Imberti, B., Morigi, M., Tomasoni, S., Rota, C., Corna, D., Longaretti, L., Rottoli, D., Valsecchi, F., Benigni, A., Wang, J., et al. (2007). Insulin-like growth factor-1 sustains stem cell mediated renal repair. *J. Am. Soc. Nephrol.* *18*, 2921–2928.
- Jackson, R., Tilokee, E.L., Latham, N., Mount, S., Rafatian, G., Strydhorst, J., Ye, B., Boodhwani, M., Chan, V., Ruel, M., et al. (2015). Paracrine engineering of human cardiac stem cells with insulin-like growth factor 1 enhances myocardial repair. *J. Am. Heart Assoc.* *4*, e002104.
- Kertesz, M., Iovino, N., Unnerstall, U., Gaul, U., and Segal, E. (2007). The role of site accessibility in microRNA target recognition. *Nat. Genet.* *39*, 1278–1284.
- Lakshmiopathy, U., and Hart, R.P. (2008). Concise review: MicroRNA expression in multipotent mesenchymal stromal cells. *Stem Cells* *26*, 356–363.
- Lam, N.N., Hung, T.D., and Hung, D.K. (2018). Acute respiratory distress syndrome among severe burn patients in a developing country: application result of the berlin definition. *Ann. Burns Fire Disasters* *31*, 9–12.
- Laroye, C., Gibot, S., Reppel, L., and Bensoussan, D. (2017). Concise review: mesenchymal stromal/stem cells: a new treatment for sepsis and septic shock? *Stem Cells* *35*, 2331–2339.
- Lee, W.Y., and Wang, B. (2017). Cartilage repair by mesenchymal stem cells: clinical trial update and perspectives. *J. Orthop. Translat* *9*, 76–88.
- Li, J., Li, S., Wang, X., and Wang, H. (2017). Esuletin induces apoptosis of SMMC-7721 cells through IGF-1/PI3K/Akt-mediated mitochondrial pathways. *Can. J. Physiol. Pharmacol.* *95*, 787–794.
- Li, J., and Zheng, J. (2019). Theaflavins prevent cartilage degeneration via AKT/FOXO3 signaling in vitro. *Mol. Med. Rep.* *19*, 821–830.
- Liu, L., Song, H., Duan, H., Chai, J., Yang, J., Li, X., Yu, Y., Zhang, X., Hu, X., Xiao, M., et al. (2016). TSG-6 secreted by human umbilical cord-MSCs attenuates severe burn-induced excessive inflammation via inhibiting activations of P38 and JNK signaling. *Sci. Rep.* *6*, 30121.
- Liu, L., Yu, Y., Hou, Y., Chai, J., Duan, H., Chu, W., Zhang, H., Hu, Q., and Du, J. (2014). Human umbilical cord mesenchymal stem cells transplantation promotes cutaneous wound healing of severe burned rats. *PLoS One* *9*, e88348.
- Martins, R., Lithgow, G.J., and Link, W. (2016). Long live FOXO: unraveling the role of FOXO proteins in aging and longevity. *Aging Cell* *15*, 196–207.

- Matthay, M.A., Pati, S., and Lee, J.W. (2017). Concise review: mesenchymal stem (stromal) cells: biology and preclinical evidence for therapeutic potential for organ dysfunction following trauma or sepsis. *Stem Cells* 35, 316–324.
- Meng, S.S., Guo, F.M., Zhang, X.W., Chang, W., Peng, F., Qiu, H.B., and Yang, Y. (2019). mTOR/STAT-3 pathway mediates mesenchymal stem cell-secreted hepatocyte growth factor protective effects against lipopolysaccharide-induced vascular endothelial barrier dysfunction and apoptosis. *J. Cell Biochem.* 120, 3637–3650.
- Menge, T., Zhao, Y., Zhao, J., Wataha, K., Gerber, M., Zhang, J., Letourneau, P., Redell, J., Shen, L., Wang, J., et al. (2012). Mesenchymal stem cells regulate blood-brain barrier integrity through TIMP3 release after traumatic brain injury. *Sci. Transl. Med.* 4, 161ra150.
- Pati, S., Gerber, M.H., Menge, T.D., Wataha, K.A., Zhao, Y., Baumgartner, J.A., Zhao, J., Letourneau, P.A., Huby, M.P., Baer, L.A., et al. (2011). Bone marrow derived mesenchymal stem cells inhibit inflammation and preserve vascular endothelial integrity in the lungs after hemorrhagic shock. *PLoS One* 6, e25171.
- Pati, S., Pilia, M., Grimsley, J.M., Karanikas, A.T., Oyenyi, B., Holcomb, J.B., Cap, A.P., and Rasmussen, T.E. (2015). Cellular therapies in trauma and critical care medicine: forging new frontiers. *Shock* 44, 505–523.
- Ren, H., Mu, J., Ma, J., Gong, J., Li, J., Wang, J., Gao, T., Zhu, P., Zheng, S., Xie, J., and Yuan, B. (2016). Selenium inhibits homocysteine-induced endothelial dysfunction and apoptosis via activation of AKT. *Cell Physiol Biochem.* 38, 871–882.
- Song, C.L., Liu, B., Diao, H.Y., Shi, Y.F., Zhang, J.C., Li, Y.X., Liu, N., Yu, Y.P., Wang, G., Wang, J.P., and Li, Q. (2016). Down-regulation of microRNA-320 suppresses cardiomyocyte apoptosis and protects against myocardial ischemia and reperfusion injury by targeting IGF-1. *Oncotarget* 7, 39740–39757.
- Temnov, A., Astrelina, T., Rogov, K., Moroz, B., Lebedev, V., Nasonova, T., Lyrshchikova, A., Dobrynya, O., Deshevoy, Y., Melerzanov, A., et al. (2018). Use of paracrine factors from stem cells to treat local radiation burns in rats. *Stem Cells Cloning* 11, 69–76.
- Tian, K.Y., Liu, X.J., Xu, J.D., Deng, L.J., and Wang, G. (2015). Propofol inhibits burn injury-induced hyperpermeability through an apoptotic signal pathway in microvascular endothelial cells. *Braz. J. Med. Biol. Res.* 48, 401–407.
- Tucka, J., Yu, H., Gray, K., Figg, N., Maguire, J., Lam, B., Bennett, M., and Littlewood, T. (2014). Akt1 regulates vascular smooth muscle cell apoptosis through FoxO3a and Apaf1 and protects against arterial remodeling and atherosclerosis. *Arterioscler Thromb. Vasc. Biol.* 34, 2421–2428.
- Walker, P.A., Shah, S.K., Jimenez, F., Gerber, M.H., Xue, H., Cutrone, R., Hamilton, J.A., Mays, R.W., Deans, R., Pati, S., et al. (2010). Intravenous multipotent adult progenitor cell therapy for traumatic brain injury: preserving the blood brain barrier via an interaction with splenocytes. *Exp. Neurol.* 225, 341–352.
- Walter, J., Ware, L.B., and Matthay, M.A. (2014). Mesenchymal stem cells: mechanisms of potential therapeutic benefit in ARDS and sepsis. *Lancet Respir. Med.* 2, 1016–1026.
- Wang, X., Zhao, Z., Gong, J., Zhou, S., Peng, H., Shatara, A., Zhu, T.Z., Meltzer, R., Du, Y., and Gu, H. (2014). Adipose stem cells-conditioned medium blocks 6-hydroxydopamine-induced neurotoxicity via the IGF-1/PI3K/AKT pathway. *Neurosci. Lett.* 581, 98–102.
- Wen, Z., Zheng, S., Zhou, C., Yuan, W., Wang, J., and Wang, T. (2012). Bone marrow mesenchymal stem cells for post-myocardial infarction cardiac repair: microRNAs as novel regulators. *J. Cell Mol. Med.* 16, 657–671.
- Wu, L., and Belasco, J.G. (2008). Let me count the ways: mechanisms of gene regulation by miRNAs and siRNAs. *Mol. Cell* 29, 1–7.
- Yan, B., and Singla, D.K. (2013). Transplanted induced pluripotent stem cells mitigate oxidative stress and improve cardiac function through the Akt cell survival pathway in diabetic cardiomyopathy. *Mol. Pharm.* 10, 3425–3432.
- Yan, P., Li, Q., Wang, L., Lu, P., Suzuki, K., Liu, Z., Lei, J., Li, W., He, X., Wang, S., et al. (2019). FOXO3-Engineered human ESC-derived vascular cells promote vascular protection and regeneration. *Cell Stem Cell* 24, 447–461.e8.
- Yang, Y., Chen, Q.H., Liu, A.R., Xu, X.P., Han, J.B., and Qiu, H.B. (2015). Synergism of MSC-secreted HGF and VEGF in stabilising endothelial barrier function upon lipopolysaccharide stimulation via the Rac1 pathway. *Stem Cell Res Ther.* 6, 250.
- Yao, Y., Jia, H., Wang, G., Ma, Y., Sun, W., and Li, P. (2019). miR-297 protects human umbilical vein endothelial cells against LPS-induced inflammatory response and Apoptosis. *Cell Physiol Biochem.* 52, 696–707.
- Yin, S., Ji, C., Wu, P., Jin, C., and Qian, H. (2019). Human umbilical cord mesenchymal stem cells and exosomes: bioactive ways of tissue injury repair. *Am. J. Transl. Res.* 11, 1230–1240.
- Yu, Y., Li, X., Liu, L., Chai, J., Haijun, Z., Chu, W., Yin, H., Ma, L., Duan, H., and Xiao, M. (2016). miR-628 promotes burn-induced skeletal muscle atrophy via targeting IRS1. *Int. J. Biol. Sci.* 12, 1213–1224.
- Zhang, X., Tang, N., Hadden, T.J., and Rishi, A.K. (2011). Akt, FoxO and regulation of apoptosis. *Biochim. Biophys. Acta* 1813, 1978–1986.
- Zhang, X., Wang, L., Peng, L., Tian, X., Qiu, X., Cao, H., Yang, Q., Liao, R., and Yan, F. (2019). Dihydromyricetin protects HUVECs of oxidative damage induced by sodium nitroprusside through activating PI3K/Akt/FoxO3a signalling pathway. *J. Cell Mol. Med.* 23, 4829–4838.
- Zhao, Y., and Srivastava, D. (2007). A developmental view of microRNA function. *Trends Biochem. Sci.* 32, 189–197.

Supplemental Information

Down-Regulation of miR-301a-3p Reduces Burn-Induced Vascular Endothelial Apoptosis by potentiating hMSC- Secreted IGF-1 and PI3K/Akt/FOXO3a Pathway

Lingying Liu, Huinan Yin, Xingxia Hao, Huifeng Song, Jiake Chai, Hongjie Duan, Yang Chang, Longlong Yang, Yushou Wu, Shaofang Han, Xiaoteng Wang, Xiaotong Yue, Yunfei Chi, Wei Liu, Qiong Wang, Hongyu Wang, Hailiang Bai, Xiuxiu Shi, and Shaozeng Li

TRANSPARENT METHODS

Cell culture

The human umbilical cord MSC (hMSC) was obtained according to the protocols as described previously (Liu et al., 2013). The human umbilical cord MSC were maintained in Mesenchymal Stem Cell Medium (MSCM, ScienCell, USA) and humidified at 37°C with 5% CO₂.

First-passage human umbilical vascular endothelial cell (HUVEC) was purchased from ScienCell Research Laboratories (ScienCell, USA). HUVEC was cultured in Endothelial Cell Medium (ECM, ScienCell, USA), and humidified at 37°C with 5% CO₂. HUVEC of passages 2-5 were used for the following experiments.

MicroRNA array analysis of severe burn induced-hMSC

The severe burn serum culture system *in vitro* was used to mimic organic microenvironment of the severe burn. Total RNAs was extracted from the hMSC, which were incubated in culture system of severe burn serum and sham serum (control) for 24h, using TRIzol (Invitrogen, USA), following the manufacturers' protocols. A miRNA array (*GeneChip miRNA Array; Affymetrix Inc., Santa Clara, CA, USA*), which contains 6153 probe sets, was used to detect the miRNA expression. miRNAs of intensities ≥ 30 were chosen for calculation. Unsupervised hierarchical clustering was analyzed by the Multi Experiment Viewer software, version 4.6 (The Institute for Genomic Research, Rockville, MD, USA). Dysregulated miRNAs were analyzed based on the following criteria: the fold change > 2 and $Q < 0.05$.

hMSC cotransfection with IGF-1 and miR-301a-3p

The hMSC (50000 cells/well) was seeded in 6-well plates with 3 mL antibiotics-free MSCM-sf. 1 day later, the cells were transfected with lentivirus-mediated overexpression vector and siRNA (negative control and IGF-1) or mimics and inhibitors (negative control and miR-301a-3p), which were synthesized by GeneChem (Shanghai, China), according to the corresponding protocol provided by manufacturers. In the first part, hMSC was divided into negative control group (un-transfected), mock group (Lenti-control transfected), IGF-1-o group (Lenti-IGF-1 transfected), mock group (Lenti-control-siRNA transfected), IGF-

1-i group (Lenti-IGF-1-siRNA transfected). In the second part, hMSC was divided to negative control group (un-transfected), mock group (Lenti-control-mimic transfected), miR-301a-3p-o group (Lenti-miR-301a-3p-mimic transfected), miR-301a-3p-o+IGF-1-o (Lenti-miR-301a-3p mimic and Lenti-IGF-1 co-transfected), mock group (Lenti-control-inhibitor transfected), miR-301a-3p-i group (Lenti-miR-301a-3p-inhibitor transfected), miR-301a-3p-i+IGF-1-i (Lenti-miR-301a-3p-inhibitor and Lenti-IGF-1-siRNA co-transfected). 12 hours later, the medium was replaced by antibiotics-free MSCM-sf. After culturing for 3-4 days, these cells were used for analysis and detection. To confirm the transfection efficiency, inverted fluorescence microscope (Leica, Germany) and flow cytometry analysis were used to detect GFP fluorescence intensity.

Dual-luciferase reporter gene assay

The binding sites of miR-301a-3p in IGF-1 was analyzed using Targetscan (www.targetscan.org) and miRanda (www.microrna.org). The wild-type (WT) and mutant (MUT) 3'-UTR of IGF-1 was cloned into luciferase expressing pMIR-REPORT vector (Ambion; Thermo Fisher Scientific, Inc.). In brief, Luciferase reporter vectors were co-transfected with mimics, antisense and corresponding mutant sequences of miR-301a-3p by Lipofectamine 2000 into 293 T cells. Luciferase activity was detected using the kit (cat. no: RG027; Beyotime Institute of Biotechnology), following the manufacturer's protocols.

Real time-PCR analysis

Total RNA was isolated from hMSC using TRIzol (Invitrogen). 2 µg of total RNA was reversely transcribed into cDNA using moloney murine leukemia virus reverse transcriptase (Invitrogen; Thermo Fisher Scientific, Inc.), according to the manufacturer's protocol. Real time-PCR was performed with SYBR Green Supermix (Bio-Rad Laboratories, Inc., Hercules, CA, USA) on the Applied Biosystems 7300 Real-Time PCR System (Thermo Fisher Scientific, Inc.). Relative level of mRNA and miRNAs was calculated using the $2^{-\Delta\Delta Cq}$ method (Livak and Schmittgen, 2001) and normalized to GAPDH and U6, respectively. The primer sequences were as following: IGF-1: Forward 5'-ACACTCCAGCTGGGAAAAGCTG GGTGAGA-3' and reverse

5'-ACACTCCAGCTGGGTCGCCCTC-3'; GAPDH: Forward
5'-TATCGGACGCCTGGTTAC-3' and reverse 5'-CGTTCAAGTTGCCGTGTC-3'.
miR-301a-3p: Forward 5'-ACACTCCAGCTGGGCAGTGCAATAGTATTGTC-3' and
reverse 5'-CTCAACTGGTGTCTGTGGA-3'; U6: Forward
5'-CTCGCTTCGGCAGCACCA-3' and reverse 5'-AACGCTTCACGAATTTGCGT-3'.

Western blotting analysis

Total proteins were extracted using RIPA buffer, supplied with Halt protease and phosphatase inhibitor cocktail (Servicebio, Wuhan, China). Proteins were separated on SDS-PAGE gel and transferred onto PVDF membranes. Then the membranes were blocked with 5% skim milk and incubated with primary antibodies at 4°C overnight. After incubated with secondary antibodies at room temperature for 3 hours and washed by PBST for three time, the protein signal on the membranes was detected using ECL-Plus kit. Primary antibodies against IGF-1, p-PI3K, PI3K, p-Akt, Akt, p-FOXO3a, FOXO3, Cleaved Caspase 3, Caspase 3 (1:1000) and β -actin (1:20,000) were from R&D Systems (Minneapolis, MN). The quantitative densitometric image analysis of the western blot images were performed using Image J software.

Co-cultured system

Transwell co-cultured system was used to investigate the paracrine effect of hMSC on severe burn-induced HUVEC apoptosis. The HUVEC in ECM were seeded to the upper chamber (0.4 μ m pore size polyester membrane from Corning, Inc.) in six-well plates (Corning, NY). The hMSC in MSCM were seeded to the lower chamber in other six-well plates (Corning, NY). They were cultured for 1 to 3 days to form a confluent monolayer. Next, the HUVEC on the upper chamber were placed to the hMSC on the lower chamber. They were simultaneously treated with DMEM-high glucose containing 20% severely burned rat serum for 24h. Finally, the hMSC and HUVEC were collected for apoptosis analysis.

Flow Cytometry assay

Apoptosis of HUVEC was analyzed using Annexin V-FITC/PI Apoptosis Detection kit I (BD, Biosciences). HUVEC and hMSC were seeded to the upper and lower chambers of co-culture system as described above. HUVEC were washed twice with PBS and

resuspended in 1×binding buffer. 1×10^5 cells in 100 uL 1×binding buffer were added with 5 uL Annexin V-FITC and 5uL propidium iodide. Flow cytometry (Becton Dickinson, USA) was used to assess the apoptotic cells.

Severely burned rat injected with hMSC that cotransfected with IGF-1 and miR-301a-3p

Six-week-old male Wistar rats (180–220g) were purchased from SPF (Beijing) Biotechnology Co., Ltd. The animals were hosted under 22 °C, 55% humidity and 12-hour light-dark cycle, fed with standard food and water ad libitum. All experimental protocols were in accordance with the International Guiding Principles for Biomedical Research Involving Animals issued by the Council for the International Organizations of Medical Sciences (CIOMS.), and approved by the Institutional Animal Care and Use Committee at the Fourth Medical Center Affiliated to PLA General Hospital.

Wistar rats (n=216) were divided into 9 groups, including Sham, Burn, Burn+hMSC, Burn+mock, Burn+IGF-1-o, Burn+IGF-1-i, Burn+miR-301a-3p-o, Burn+miR-301a-3p-i and miR-301a-3p-i+IGF-1-i. Each group was divided equally into three subgroups of 8 rats at 12h, 24h, 48h after severe burn. Rats were anesthetized by intraperitoneal injection of 300 mg/kg Avertin (20 mg/ml) (2,2,2-tribromoethanol, Sigma, USA). Both whole backside and abdomen were placed in hot water (94°C) for 12s and 6s, respectively, which caused 50% TBSA with a full-thickness burn. Intraperitoneal injections of balanced salt solution (40 ml/kg) were immediately administered to prevent shock.

The rats in the Burn+mock, Burn+IGF-1-o, Burn+IGF-1-i, Burn+miR-301a-3p-o, Burn+miR-301a-3p-i and miR-301a-3p-i+IGF-1-i groups immediately received a tail vein injection of 5×10^6 hMSC, which were transfected with Lenti-GFP-vehicle, Lenti-IGF-1-overexpression, Lenti-IGF-1-siRNA, Lenti-miR-301a-3p mimic, Lenti-miR-301a-3p inhibitor and Lenti-miR-301a-3p-i inhibitor combined Lenti-IGF-1-i-siRNA. The rats in the Burn+hMSC group immediately received 5×10^6 hMSC by tail vein injection. And the rats in sham and burn groups received PBS by tail vein injection. The burn wound was treated with 1% tincture of iodine and kept dry to avoid infection.

Pulmonary function test (PFT)

Pulmonary function test (PFT) can provide a simple noninvasive method of assessing airway compromise. At 24h after severe burn, pulmonary function was measured by AniRes2005 animals lung function detector, then data were assayed using AniRes2005 software (Beijing Bestlab High-Tech Co.,Ltd, China).

Specimen collection and detection

The blood samples were collected from aortavertralis at 12h, 24h and 48h post burn injury or sham injury, and serum were used for the ELISA assay and blood biochemical detection, as well as serum at 24h post burn for building the severe burn serum culture system *in vitro*. Meanwhile, organs including lung, liver, kidney and heart samples were collected for immunofluorescence staining and permeability detection, and their tissues supernatant were used for the ELISA assay. The 24 hours urine volume in each group was collected using metabolic cage and recorded. The metabolic cages (Nalgene, Thermo Fisher) consist of a circular upper portion, which houses the rat; a wire-grid floor (diameter, 21.5 cm; approximate surface area, 363 cm²; opening, 1×3.1 cm); and a lower collection chamber with a specialized funnel that separates fecal pellets and urine that fall through the grid floor for their collection into 2 separate tubes (diameter, 4 cm; Nalgene, Thermo Fisher).

Blood biochemical detection

The serum biochemical parameters, including alanine transaminase (ALT), aspartate transaminase (AST), urea (Urea) and creatinine (Crea), troponin, creatine kinase (CK), MB isoform of CK (CK-MB), lactate dehydrogenase (LDH), α -hydroxybutyrate dehydrogenase (HBDH) were measured at the Central Institute of Clinical Chemistry and Laboratory Medicine of the Fourth Medical Center Affiliated to PLA General Hospital.

Dual immunofluorescence staining

The lung, liver, kidney and heart samples were fixed with 4% paraformaldehyde and embedded in paraffin. 5 μ m sections were deparaffinized, rehydrated, and stained with immunofluorescence according to standard procedures. In brief, the sections were labeled with 1:50 monoclonal mouse against human MSC FITC-CD105 antibody (Abcam, USA) and monoclonal rabbit against rat endothelial CD31 antibody (Abcam, USA) at 4°C. Next, 1:500 Alexa Fluor 594 AffiniPure Goat Anti-Rabbit IgG secondary antibody was used. In

addition, other sections were stained by One Step TUNEL Apoptosis Assay Kit (Beyotime, China) and monoclonal rabbit against rat endothelial CD31 antibody (Abcam, USA), followed by incubation with the CD31 secondary antibody. Finally, 500 μ L 4,6-diamidino-2-phenylindole (DAPI) was used for nuclear staining (green-TUNEL+red-CD31-VEC+blue-DAPI-nuclear). Cover sheets were glued on the glass slides with anti-fluorescence quenching sealant and observed with a laser scanning confocal microscope (Guo et al., 2018).

Vascular permeability assay

Evans blue (EB) was applied to detect the vascular permeability of tissues or organs. 2% EB (2 ml/kg, Sigma, St. Louis, MO, USA) was intravenously administered into the rats. 1h later, the rats were anesthetized and transcatheterially perfused with 0.9% NaCl. The organs were removed and immersed in formalin (10 ml/kg, Sigma, St. Louis, MO, USA) at 60°C for 24h. The organs were ground and centrifuged at 4°C. OD₆₃₂ was measured on an automatic microplate reader (BioTek, USA). Organs were collected for wet weight (WW) and dry weight (DW) measurement. Water content ratio of vital organ tissues was calculated as $(WW-DW)/WW \times 100\%$ (Chai et al., 2013).

Enzyme-linked immunosorbent assay (ELISA)

The IGF-1 level in cultural supernatant of hMSC and in serum, organ tissues of severely burned rats was examined with a double-antibody sandwich ELISA kit (eBioscience, USA) following the manufacturer's instructions. The OD value was detected on a multi-detection microplate reader.

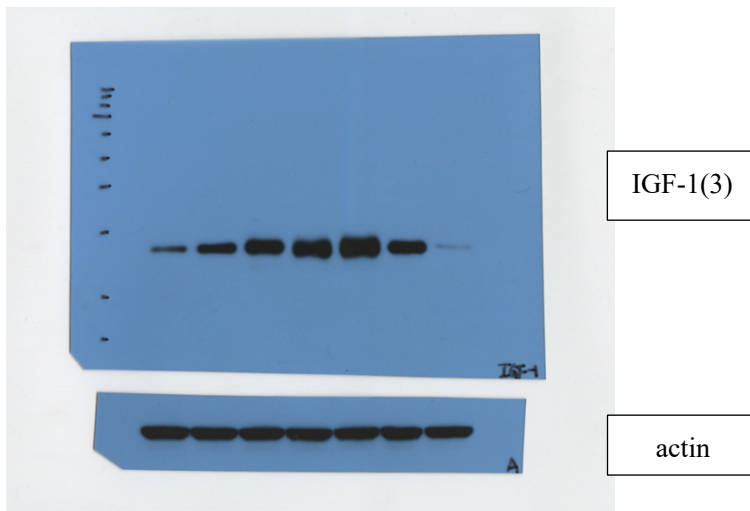
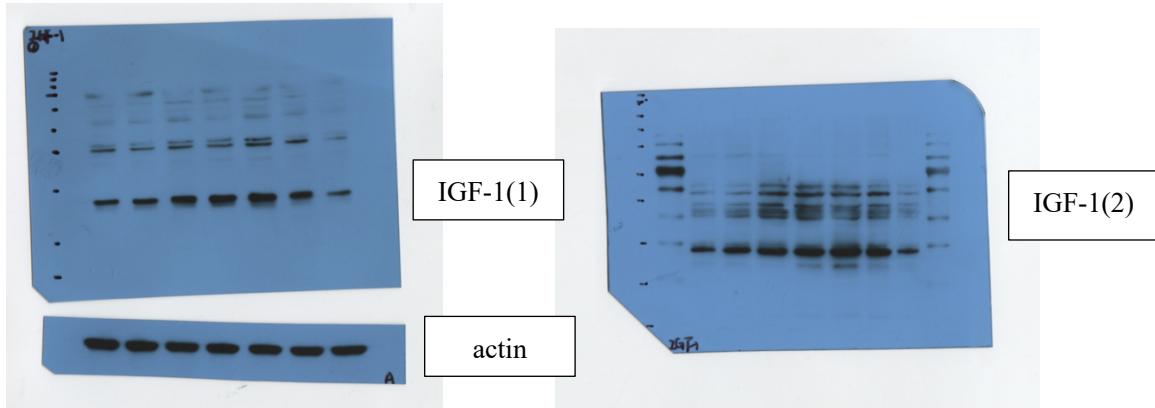
Statistical analysis

The data shown as the mean \pm SD ($\bar{x} \pm s$) were analyzed by SPSS 18.0 (SPSS Inc., Chicago, IL, USA). Statistical difference was analyzed using one-way ANOVA and multiple comparisons were performed using Student-Newman-Keuls tests. Statistical difference was considered significant when $p < 0.05$.

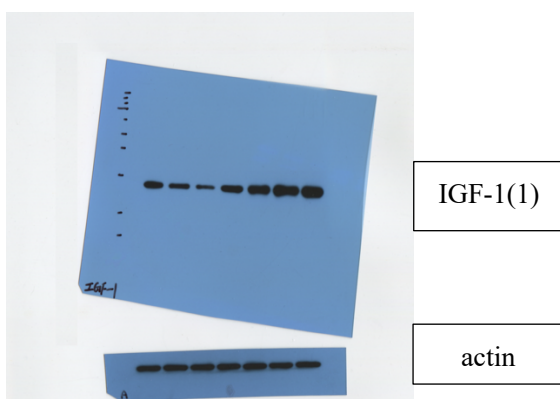
Supplemental figures

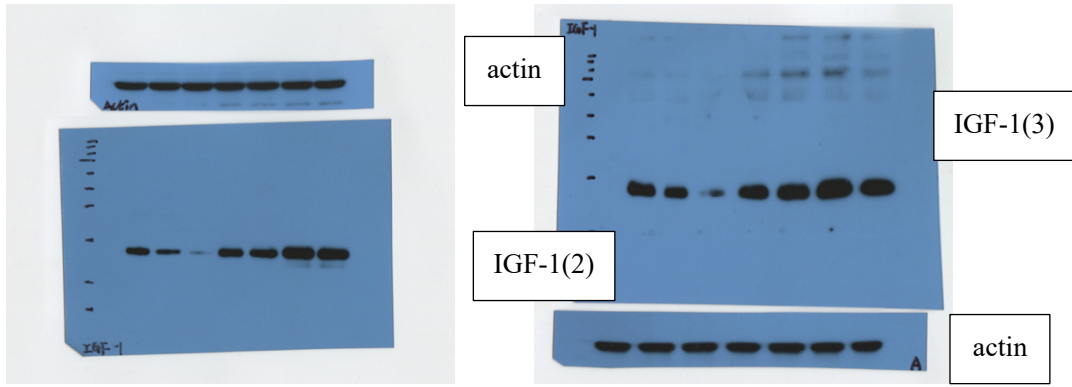
Data S1: Full unedited blots for Fig1E, Fig 3E, Fig 6A and Fig 6B, each experiment was repeated for 3 times.

Full unedited blots for Fig 1E

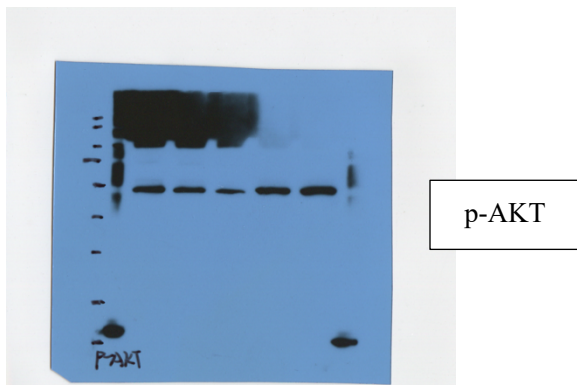
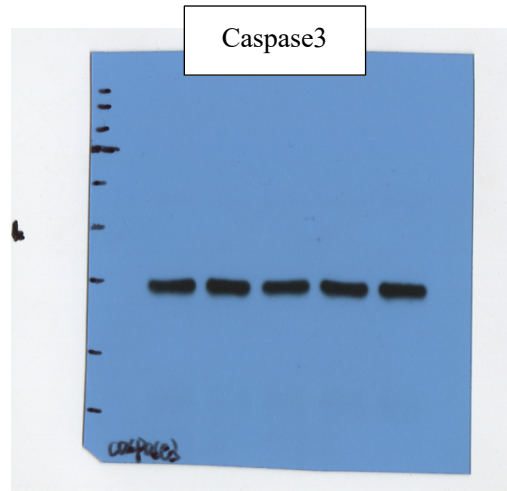
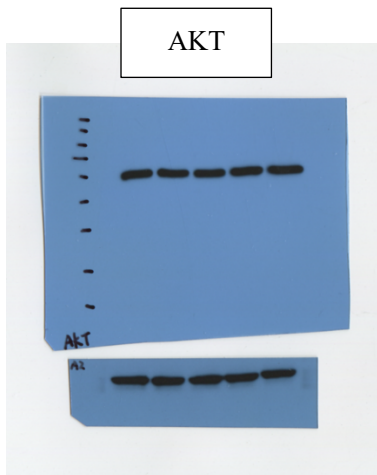


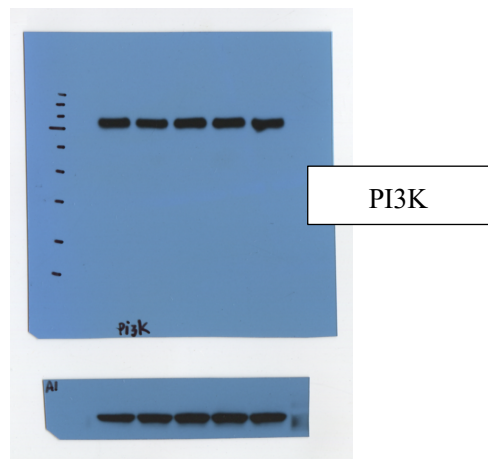
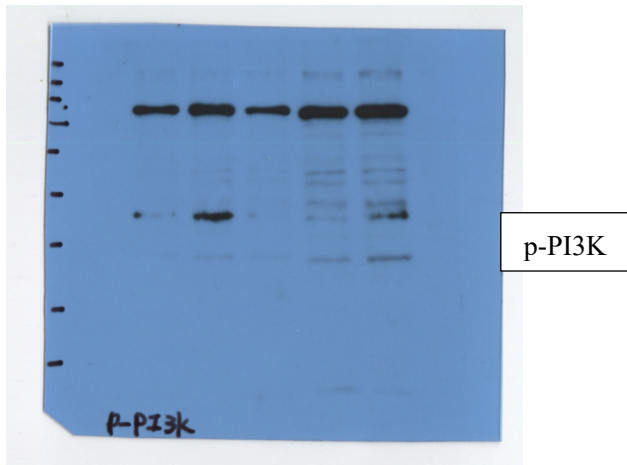
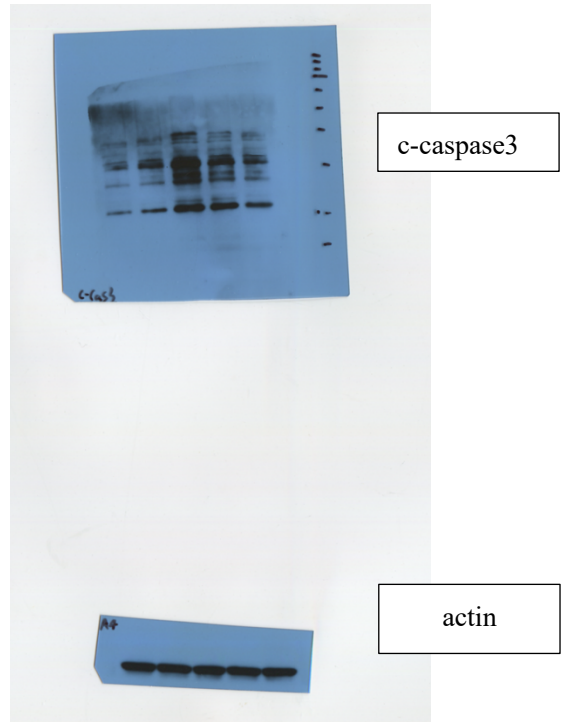
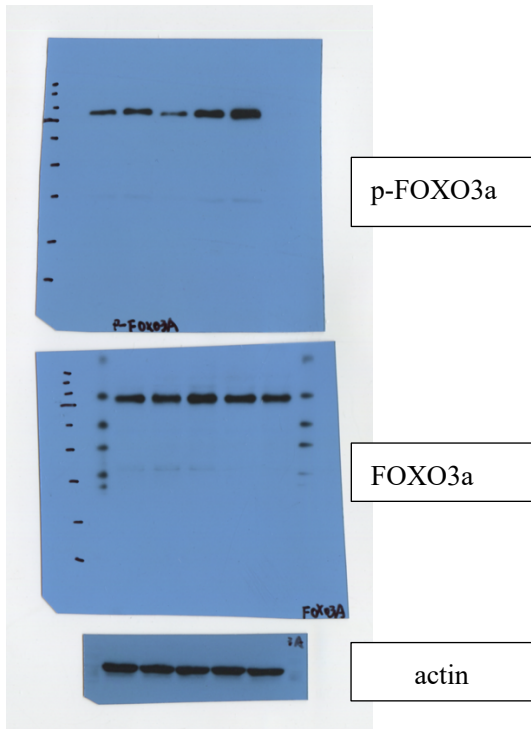
Full unedited blots for Fig 3E



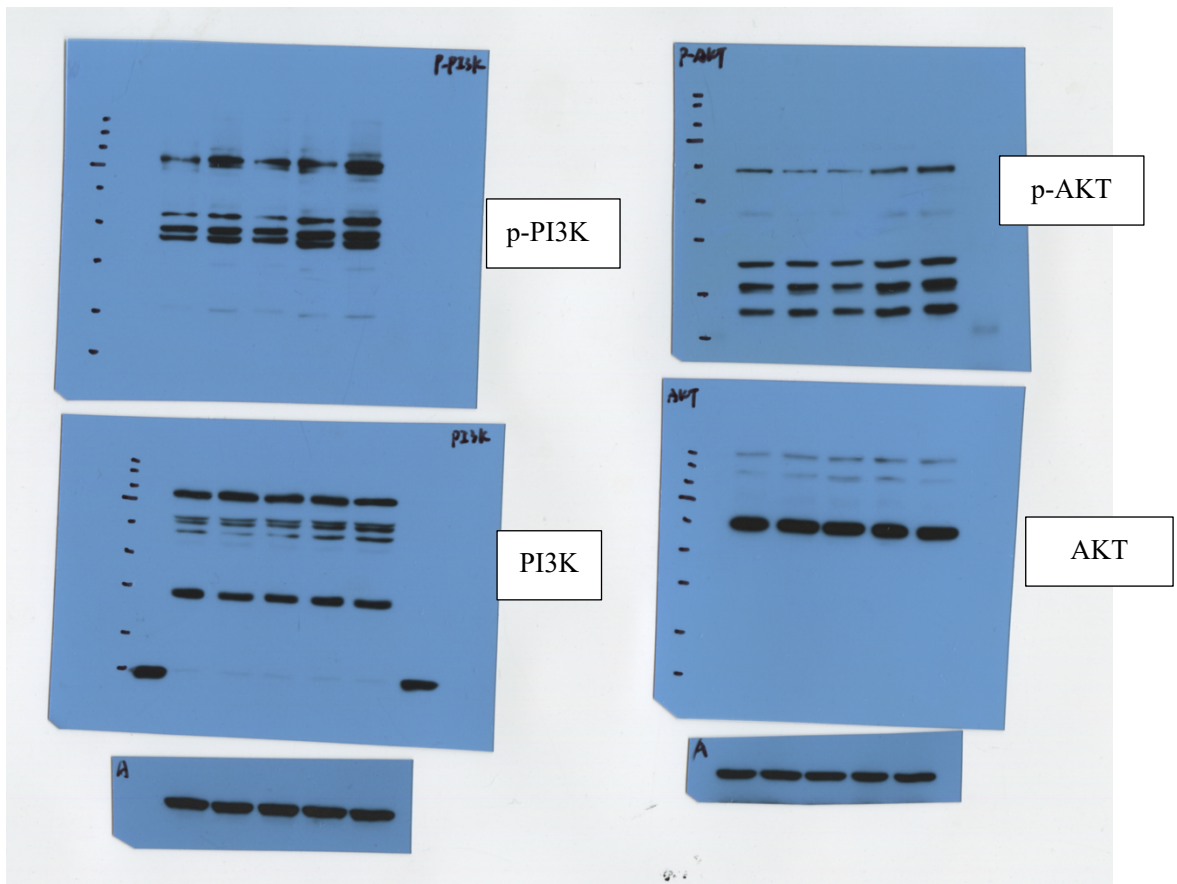


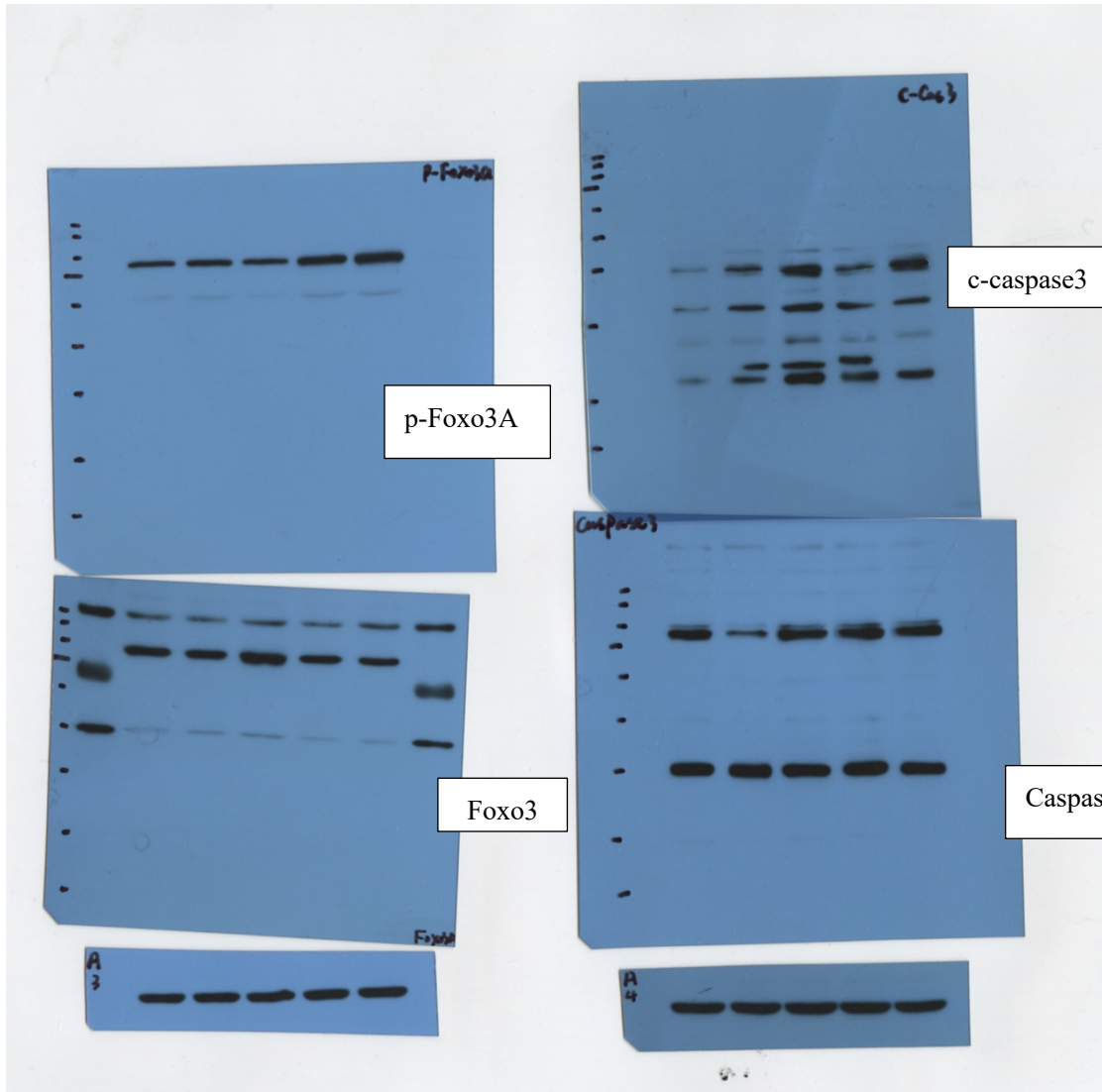
Full unedited blots for Fig 6A PI3K signal (1)



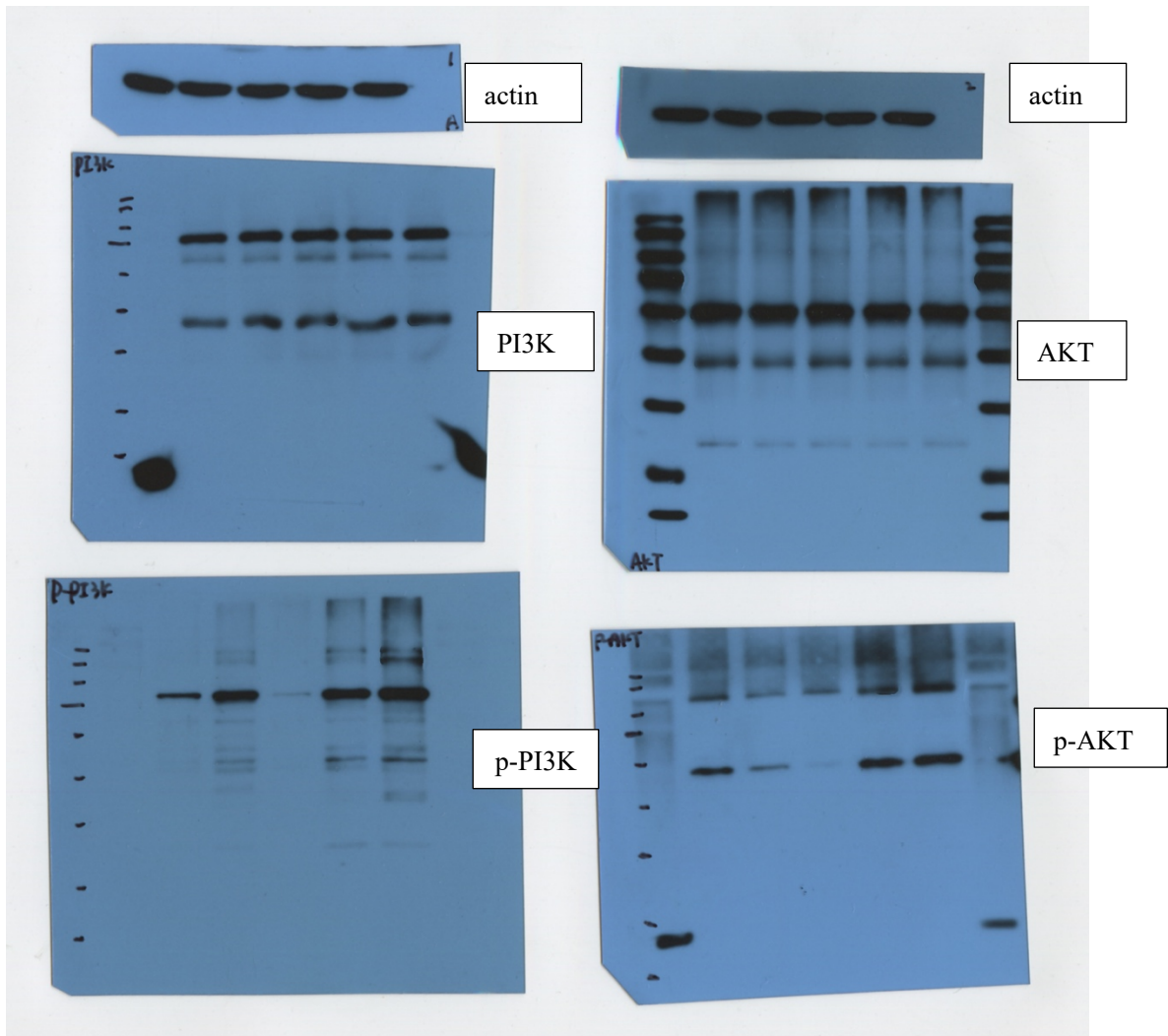


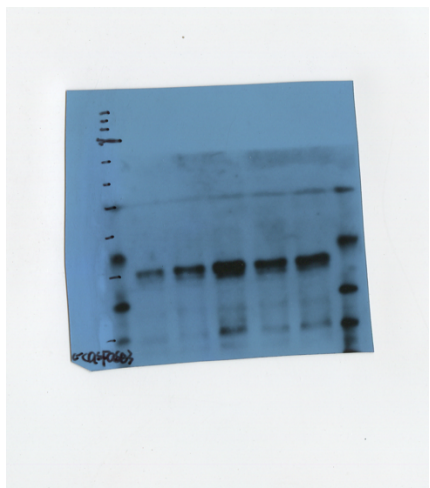
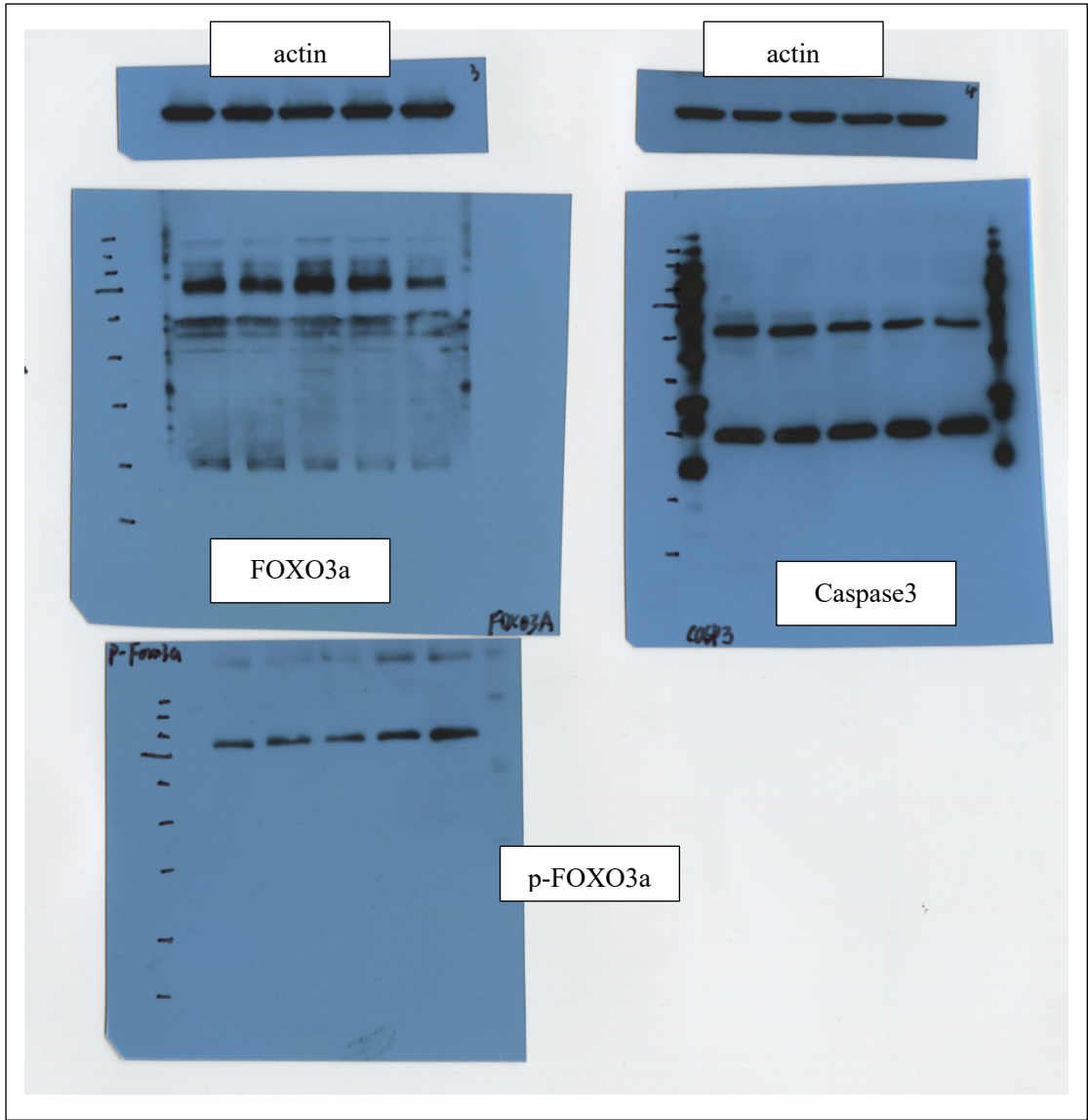
Full unedited blots for Fig 6A PI3K signal (2)





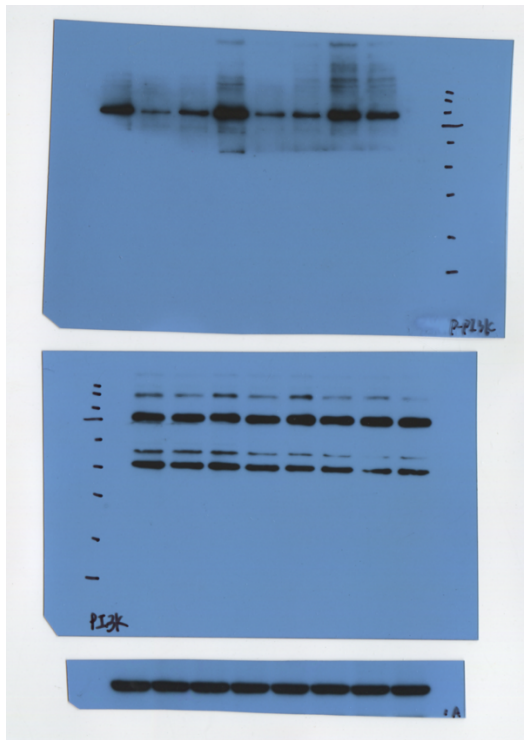
Full unedited blots for Fig 6A PI3K signal (3)





c-caspase3

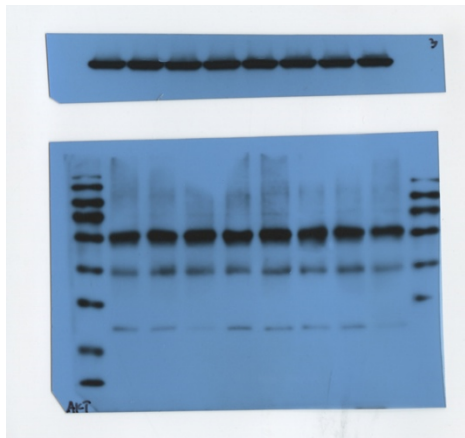
Full unedited blots for Fig 6B (1)



p-PI3K

PI3K

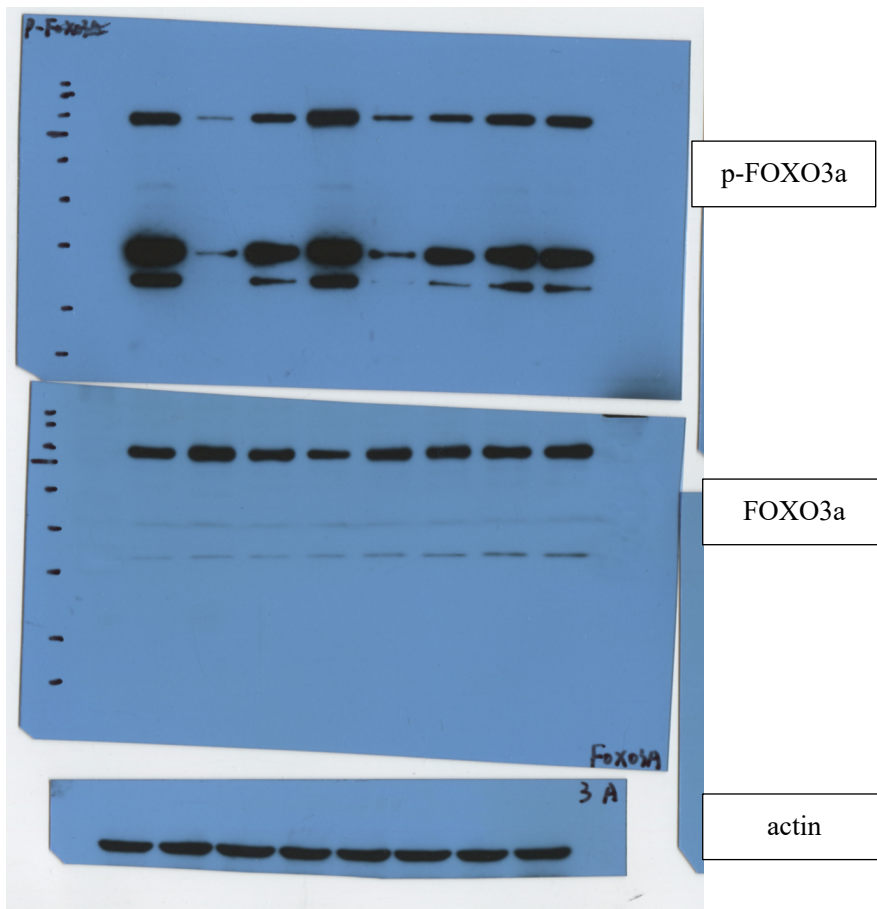
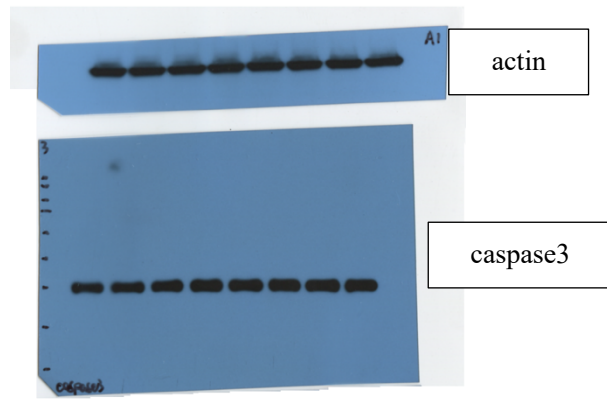
actin



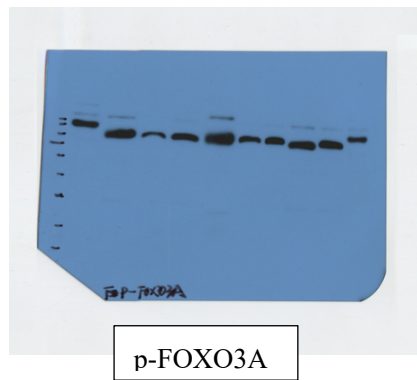
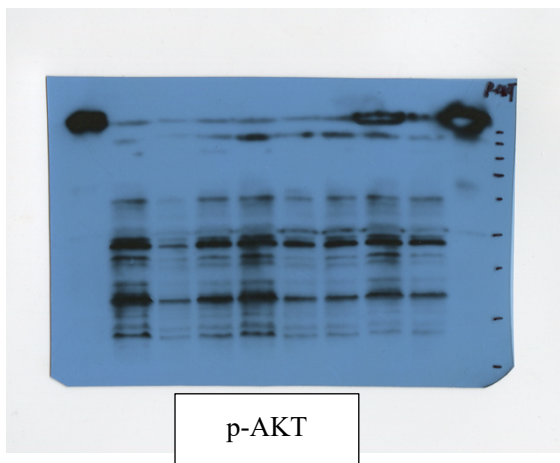
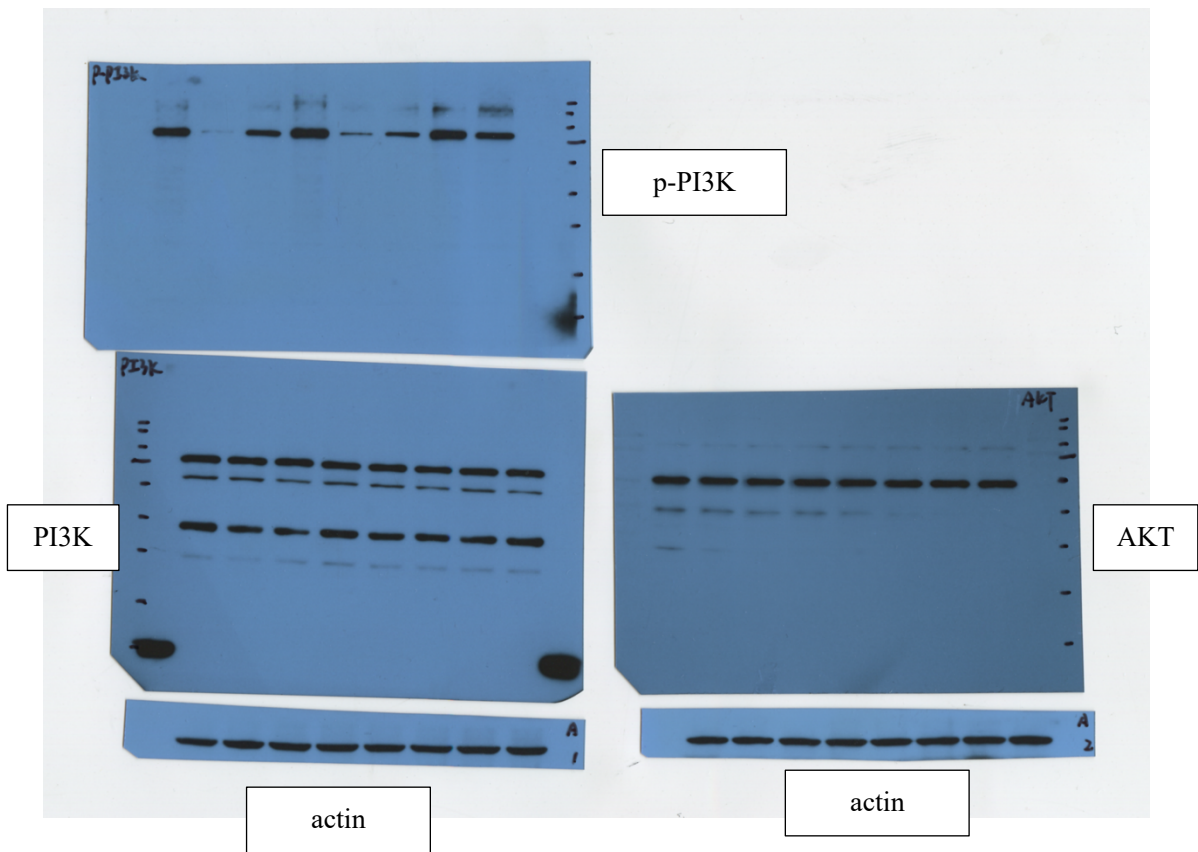
AKT

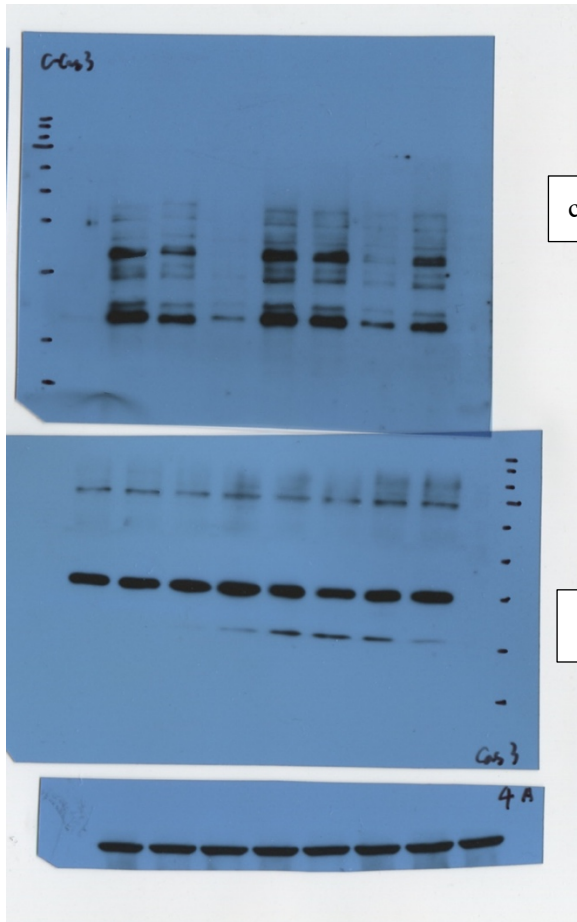


p-AKT



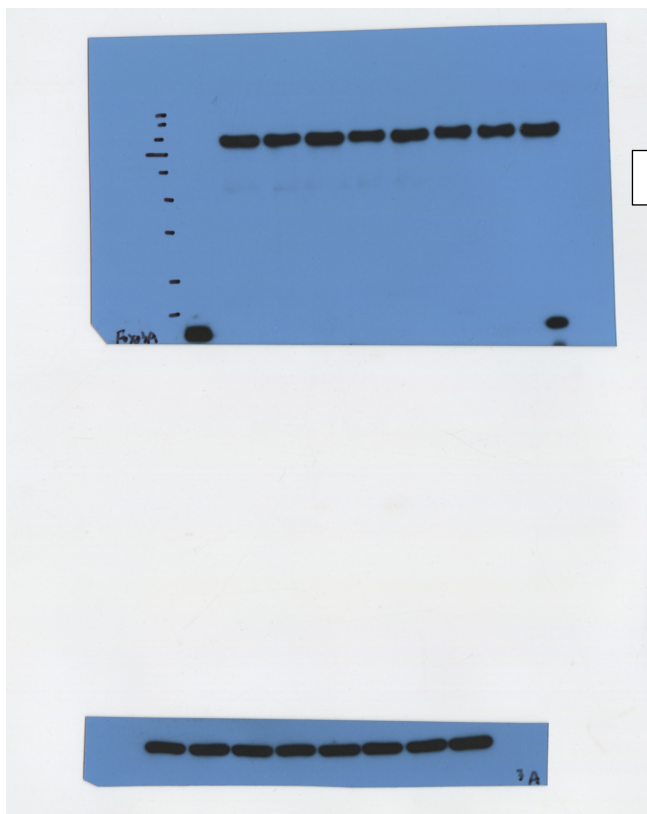
Full unedited blots for Figure 6B (2)





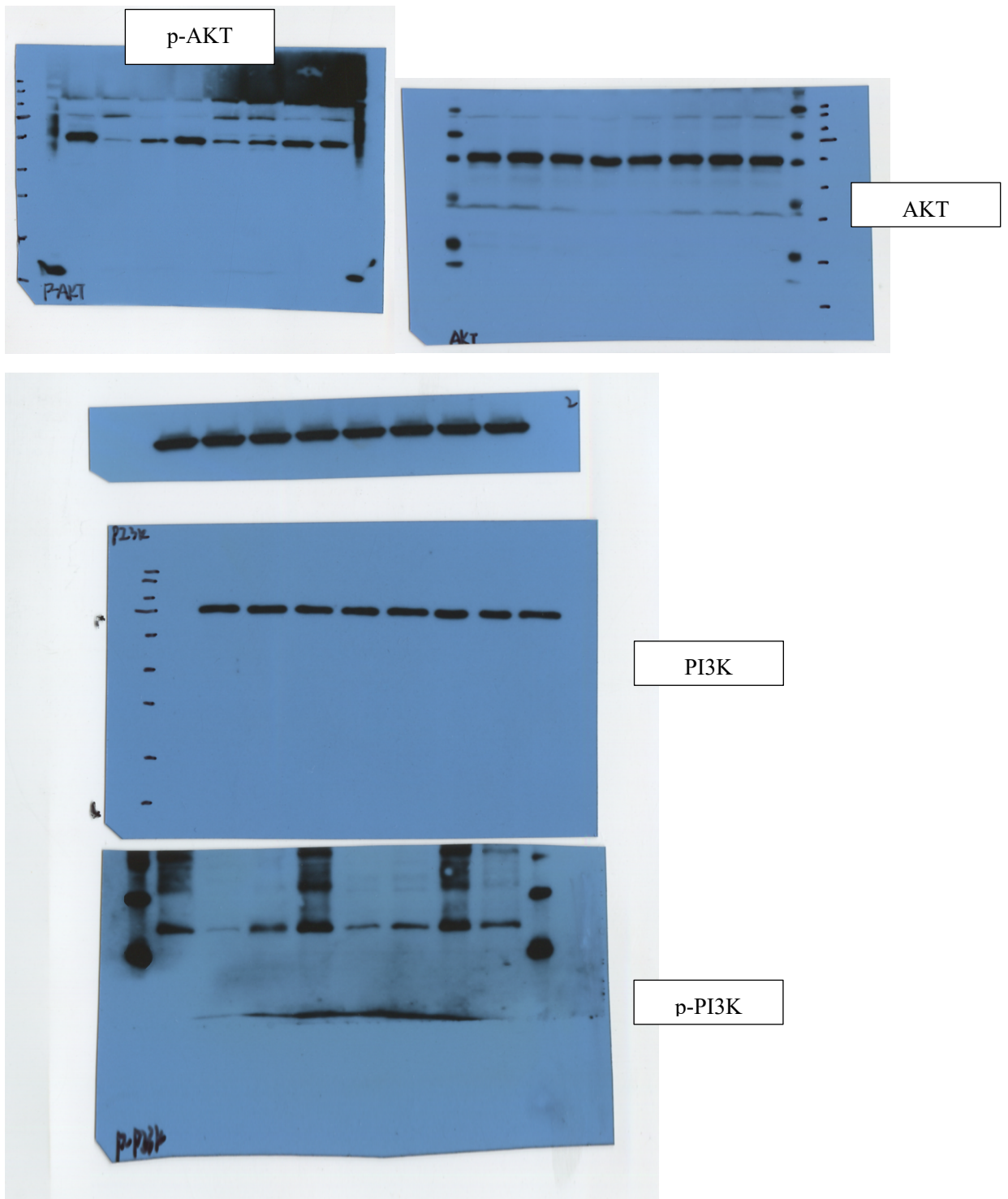
c-caspase3

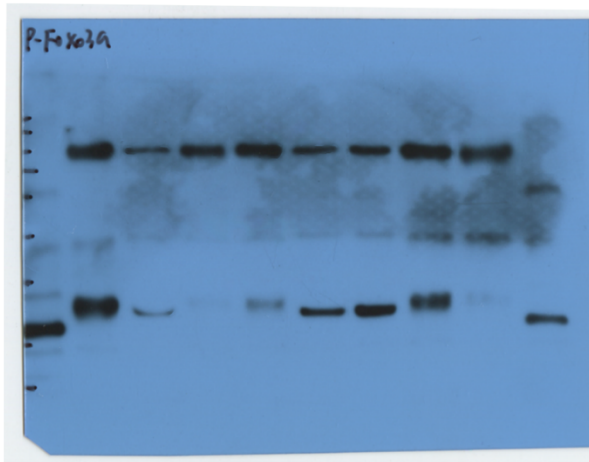
caspase3



Foxo3a

Full unedited blots for Figure 6B (3)





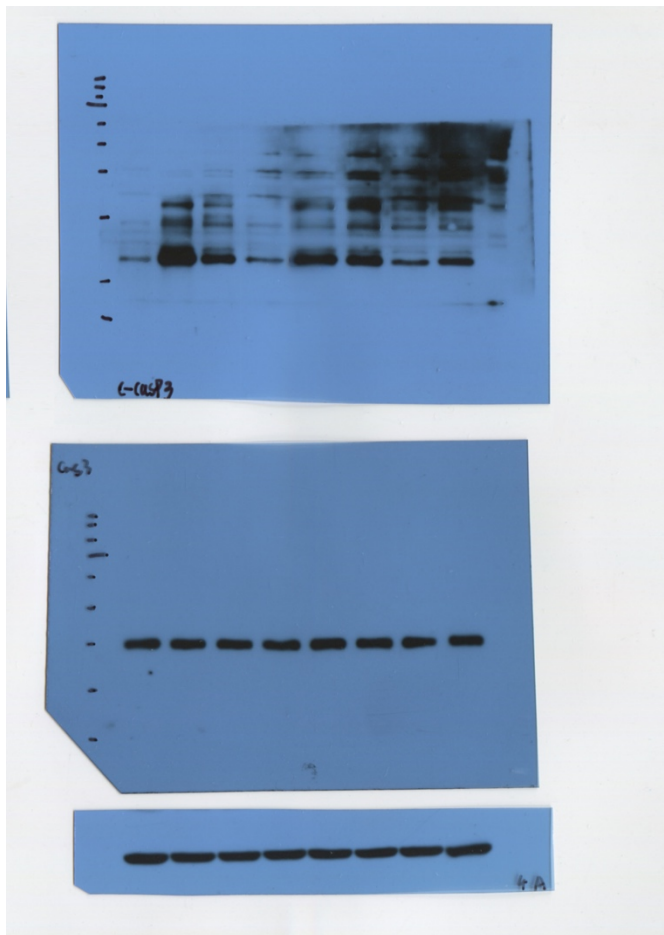
p-FOXO3a



actin



FOXO3a



c-caspase3

caspase3